# Genome-wide RAD sequencing data suggest predominant role of vicariance in Sino-Japanese disjunction of the monotypic genus *Conandron* (Gesneriaceae)

Shao-Jun Ling[1,4], Xiao-Lan Yao[1,4], Juli Caujapé-Castells[2], Jordi López-Pujol[3], Ke Tan[1,4,*], Ming-Xun Ren[1,4,*]

[1] Ministry of Education Key Laboratory for Genetics and Germplasm Innovation of Tropical Special Forest Trees and Ornamental Plants, Hainan University , Haikou 570228, China

[2] The Jardín Botánico Canario "Viera y Clavijo"-UA CSIC (Cabildo de Gran Canaria), 35017 Las Palmas de Gran Canaria, Spain

[3] Botanic Institute of Barcelona (IBB, CSIC-Ajuntament de Barcelona), 08038 Barcelona, Spain

[4] Center for Terrestrial Biodiversity of South China Sea, Hainan University, Haikou 570228, China

* Correspondence author: Ke Tan, Email: tanke@hainanu.edu.cn); Ming-Xun Ren, Email: renmx@hainanu.edu.cn

# Genome-wide RAD sequencing data suggest predominant role of vicariance in Sino-Japanese disjunction of the monotypic genus *Conandron* (Gesneriaceae)


## Abstract

Disjunct distribution is a key issue in biogeography and ecology, but it is often difficult to determine relative roles of dispersal *vs.* vicariance in disjunctions. *Conandron ramondioides* (Gesneriaceae) is a tertiary relict monotypic species distributed disjunctively in mainland China, Taiwan Island and Japan, where is a key region for understanding evolution and diversification of modern angiosperms. Population phylogenetic and phylogeographic structures of a comprehensive sampling of *C. ramondioides* by ddRAD sequencing were assessed, combined ABC modeling and SDM to infer the effects of multiple glaciation periods and to survey climatic niche differences by checking putative population divergence models and demographic scenarios. We found a very high degree of genetic differentiation among mainland China, Taiwan Island and Japan, with very limited gene flow between regions and a clear Isolation by Distance pattern. Mainland China and Japan clades diverged first from a widespread ancestral population in middle Miocene, followed by a later divergence between mainland China and Taiwan Island clades at early Pliocene. Three current groups have survived in various glacial refugia during LGM, and experienced contraction and/or bottlenecks since their divergence during Quaternary glacial cycles, with strong niche divergence between mainland China + Japan and

Taiwan Island ranges. Overall, we verified a predominant role of vicariance in the current disjunction of monotypic genus *Conandron*. The sharp phylogenetic separation, ecological niche divergences among these three groups and the great number of private alleles in all populations sampled indicate a considerable time of independent evolution, and suggests the need of a taxonomic survey to detect potentially overlooked taxa.

**KEYWORDS**

Demography; isolation by distance; species distribution model; phylogeography; ecological niche differences

# 1 INTRODUCTION

Due to its vast extension, stretching from boreal to tropical ecosystems, East Asia is a key region for relict species/lineages which survived Cenozoic climatic deterioration, and thus often presents complicated species distribution patterns, e.g., disjunctions (Qiu et al., 2009, 2011; Qi et al., 2014; Tang et al., 2018). Traditionally, two alternative explanations have been proposed to explain species disjunct distributions (Tallis, 1991), i.e. long-distance dispersal across preexisting geographical barriers, or the fragmentation of a widespread ancestral range (vicariance) by the formation of geographical barriers such as mountain uplifts and marine transgressions. The role of dispersal versus vicariance has fascinated scientists in the fields of biogeography and evolutionary ecology for decades, but the relative contribution of these diversification

64 forces to current species geographic patterns is still debated, partly due to the
65 elusiveness of extinction and the high number of biotic, abiotic and stochastic factors
66 that overlap throughout the geological ontogeny of each region (Caujapé-Castells et
67 al., 2017).

68 *Conandron ramondioides* Siebold & Zucc. is the only species of genus
69 *Conandron* (Gesneriaceae), with a disjunct distribution in mainland China (in four
70 provinces, Anhui, Fujian, Jiangxi, and Zhejiang), Taiwan Island, and the Japanese
71 islands (Honshu, Kyushu, Shikoku, and the Ryukyus) (Wang, 2004; Wang et al., 2010;
72 Xiao et al., 2012). This monotypic genus is distinctive for its radially symmetrical
73 corolla with four fertile stamens and cohesive anthers (Wang et al., 2010). The
74 molecular data available indicate that *C. ramondioides* is a relict taxon and probably
75 split from its closest relatives ca. 30 Ma (Roalson & Roberts, 2016), making it
76 phylogenetically distinct from other taxa in the Old World Gesneriaceae (Wang, 2004;
77 Wang et al., 2010; Weber, 2004; Roalson & Roberts, 2016). Although several studies
78 had explored the population differentiation of its Chinese populations with DNA
79 markers (Xiao, 2005; Xiao et al., 2012), a detailed study sampling the whole range
80 (including mainland China, Taiwan Island, and Japan) using updated molecular
81 methods is still needed to explore the processes underlying its phylogenetically
82 isolated condition within the Gesneriaceae and the evolutionary history of plant
83 disjunctions in this species-rich region.

84 Here, we use restriction site-associated DNA sequencing (RAD-seq) on an
85 extensive sampling of *C. ramondioides* in mainland China, Taiwan Island and

Japanese islands, to investigate its phylogeographic structure and (putative) genetic barriers, population divergence models and demographic scenarios, and to evaluate the effects of past climate changes on distribution ranges and test for ecological niche differentiations, with final note about the role of dispersal versus vicariance in the shaping of current East Asia flora.

# 2 MATERIAL AND METHODS

## 2.1 Sampling and DNA extraction

*C. ramondioides* is a perennial and rhizomatous herb usually grows on wet and moss-covered granite rocks in mountain cliffs and valleys (Wang, 2004; Xiao et al., 2012). Its local populations are usually highly fragmented and restricted to isolated mountain areas (Wang, 2004; Xiao, 2005). We sampled a total of 11 populations of *C. ramondioides* covering its whole distribution range as described in *Flora of China* (Hu & Kelso, 1996) and *Flora of Japan* (Iwatsuki et al., 1993) (Table 1). All samples were dried and stored in silica gel in the field. Voucher specimens were deposited in the Herbarium of Hainan University (HUTB; Table 1). A total of 108 individuals of *C. ramondioides* were sampled and studied, with three individuals of *Ridleyandra* (phylogenetically close to *Conandron*, Roalson & Roberts, 2016) used as outgroup. The total genomic DNA was extracted from young leaves using a modified CTAB protocol adapted from Doyle & Doyle (1987). The DNA quality was assessed with a 1.0% agarose gel.

## 2.2 RAD library preparation and sequencing

A total of 100 ng genomic DNA of each individual was digested with two restriction enzymes, *EcoR*I and *Pst*I (New England Biolabs, Beverly, USA) at 37°C for 8 h. The restriction enzymes were then inactivated by heating at 65°C for 20 min. After ligation with individually barcoded *Eco*RI adapter and universal *Pst*I adapter with T4 DNA ligase for each sample at 16°C for 8 h, the reaction was stopped by heating at 65°C for 20 min. The ligation products of 24 samples were equally pooled and size-selected into 300–500 bp fragments using the agarose gel electrophoresis. After the gel purification step, the derived fragments were used as templates (about 30 ng) for PCR amplification via 25 cycles with *Eco*RI and *Pst*I adapter universal primers using PrimeStar Max DNA Polymerase (Takara, Dalian, China). Finally, the amplicons were size-selected once more into 350–500 bp fragments with the method mentioned above. The resulting ddRAD library was sent to Guangzhou Jierui Biotechnology Company (Guangzhou, China) and sequenced on the Illumina NovaSeq platform using 150 nt with paired end mode.

### 2.3 *De novo* clustering and SNP exploitation

We used the *process_radtags* module in the Stacks v2.4 program (Catchen et al., 2013) to de-multiplex the raw data, setting all parameters as default. We also trimmed all the reads to 135 bp in length to remove low quality nucleotides at the 3′ end of each read. Each end of the retained reads was treated as an independent locus, and we combined all of them for the statistical analyses. We first used the *ustacks* module in Stacks to cluster the reads into exactly-matching stacks. Here we set $m = 2$ as the minimum depth of coverage ($m$) and $M = 12$ as the maximum distance allowed between stacks

within an individual. We then used the *cstacks* module to build the catalogs for all 111 individuals with $n$ = 12 as the maximum number of mismatches allowed between individuals. The *sstacks* module was used to generate alignment results for each individual against the catalog using default parameters. In the populations module, we set $p$ = 10 and $r$ = 0.6 to call the consensus SNPs among 108 individuals, which requires SNPs to be found in at least eight populations and 60% individuals within one population. The *phylip*, *structure* and *vcf* files were generated and the data were filtered using VCFtools (Danecek et al., 2011) for subsequent analysis. PGDspider v2.02 (Lischer & Excoffier, 2012) was used subsequently for file conversion to program-specific formats.

**2.4 Population genetic structure and phylogeny**

Genetic summary statistics for ddRAD-seq genomic data, including the percentage of polymorphic sites (%$P$), observed and expected heterozygosity ($H_O$ and $H_E$), nucleotide diversity ($\pi$), and inbreeding coefficient ($F_{IS}$), were estimated using *populations* in *Stacks* for all populations (11) with more than five samples. Pairwise $F_{ST}$ values were calculated using Arlequin v3.5.2.2 (Excoffier & Lischer, 2010), with 10,000 permutations. Hierarchical analysis of molecular variance (AMOVA) was implemented based on our assessment the hierarchical population structure ($K$ = 2 and $K$ = 3, see Results and Discussion) in order to quantify genetic variation partitioning across the different sampling levels.

To evaluate admixture in all populations of *C. ramondioides*, we used the maximum likelihood method implemented in ADMIXTURE v1.3.0 to estimate

individual admixture (Alexander et al., 2009; Decker et al., 2014). This method allowed for uncertainty in ancestral allele frequencies. We predefined the number of populations as $K = 1$ to $K = 12$. Ten independent runs were performed for each value of $K$. The optimal $K$ was chosen using the lowest cross-validation (CV) error.

We further performed a Principal Components Analysis (PCA) to visualize the major axes of genetic variation using the *Adegenet* package (*glPCA* function; Jombart, 2008) in R. Then we used *ggplot2* to plot the PCA, color the samples by population, and create ellipses that include 95% of the data for each the population.

Finally, we estimated a maximum-likelihood phylogeny of the 11 populations from unlinked SNPs with a GTR substitution matrix and GAMMA model using RAxML 8.2.6 (Stamatakis, 2006). Three individuals of *Ridleyandra* were used as outgroups. Nodal support was estimated using 1000 bootstrap replicates.

**2.5 Genetic differentiation and geographical distance**

To investigate the correlation between genetic and geographic distances, we used GenAlEx v6.5 to perform a Mantel test at the population level. The genetic distance matrix was obtained from the pairwise $F_{ST}$ values calculated by Arlequin v3.5.2.2 (Excoffier & Lischer, 2010), and the geographic distance matrix (i.e. the straight-line distances between each possible population pair) was generated from the latitude and longitude coordinates.

In order to determine the occurrence of gene exchange barriers along the species range, we used Barrier v2.2 (Manni et al., 2004) to identify the areas of maximum variation between populations according to Monmonier's (1973) maximum-difference

algorithm. The genetic distance matrix ($F_{ST}$) between two populations and the latitude and longitude data of each population were imported into the software, and the number of barriers was set to 3.

### 2.6 Estimates of historical demography

We employed DIYABC v2.1.0 software to explore the historical demography of *C. ramondioides*, which uses an Approximate Bayesian Computation (ABC) algorithm (Cornuet et al., 2014). Based on the results of ADMIXTURE, PCA, and phylogenetic tree of *C. ramondiodes*, the 11 studied populations were classified into three groups, i.e. group MC (mainland China), group TW (Taiwan Island) and group JP (Japan). The JP clade was located at the base of phylogenetic tree, thus we first tested six possible divergence scenarios to estimate whether *C. ramondiodes* originated from Japanese islands (Figure S3A). We selected a single SNP per locus, which had to be present in at least 70% of the individuals in all three groups. The simulated SNP dataset was obtained by the algorithm proposed by Hudson (2002). A uniform prior probability was employed, and all summary statistics were selected to generated a reference table, based on $6 \times 10^6$ simulated datasets. To estimate the relative posterior probabilities for each scenario, we used 1% simulated datasets closest to the observed data to obtain logistic and posterior distribution of historical demographic parameters according to the most likely scenario (Cornuet et al., 2010). A conservative estimate for generation time to 3 years to estimate the demographic history of *C. ramondiodes* was set, based on our field observations. In order to choose the best fit demographic scenario and parameter estimation, surveys in the three groups of *C. ramondiodes*

were carried out by using four models of changes in population size with same parameter settings (Figure S3B).

**2.7 Species distribution models**

Species distribution models for *C. ramondioides* for the Last Interglacial period (LIG, ca. 120,000 years BP), Last Glacial Maximum (LGM, ca. 21,000 years BP), current and future (year 2070) periods, were generated using MaxEnt v3.4.1 (https://biodiversityinformatics.amnh.org/open_source/maxent/; Phillips et al., 2006). In addition to our sampling sites, the distribution records for *C. ramondioides* sourced from Global Biodiversity Information Facility (GBIF, http://www.gbif.org), Chinese Virtual Herbarium (http://www.cvh.org.cn) and National Specimen Information Infrastructure (NSII, http://www.nsii.org.cn/) were also included; in total, 74 *C. ramondioides* occurrence sites were acquired to build the models (Table S3). Duplicate records within 30″ × 30″ cells were removed to reduce the effects of spatial autocorrelation under different climate variations. The bioclimatic layers for the LIG (Otto-Bliesner et al., 2006), current and future (Community Climate System Model Version 4, CCSM4; Gent et al., 2011) climate data were retrieved from the WorldClim 1.4 website (http://www.worldclim.org; Hijmans et al., 2005) at 30″ spatial resolution (approximately 1 $km^2$ on the ground). The year 2070 model was run under RCP 8.5, which represents the highest emission scenario (an increase of 2.6–4.8 ºC; Collins et al., 2013). For the LGM, we took data from three climatic models offered by the WorldClim website, CCSM4, the Model for Interdisciplinary Research on Climate (MIROC, Watanabe et al., 2011) and the New Earth System Model of the Max Planck

Institute for Meteorology (MPI-ESM-P: http://www.mpimet.mpg.de/en/science/models/mpi-esm/), at a scale of 2.5′ × 2.5′ (which were later resampled to 30″ resolution). Nine uncorrelated and biologically significant bioclimatic variables were selected as predictors (Table 4), after Pearson correlation coefficients (*r*) analysis of each pairwise comparison of 19 bioclimatic variables. Model validation was carried out using default settings with 10 bootstrap replicates and 10,000 background points of cross-validation procedures with 25% of the point data used for model testing. The contribution of each variable was assessed by the jackknife approach (Baldwin, 2009), and the performance of each model was evaluated by the receiver operating characteristic curve (AUC; Fielding & Bell, 1997; Wang et al., 2007), with value >0.9 indicating good prediction (Swets, 1988). The MaxEnt results were categorized into highly suitable area (0.75–1.00), moderately suitable area (0.50–0.75), lowly suitable area (0.25–0.50) and unsuitable area (0–0.25) based on logistic probability values.

**2.1.8 Niche comparisons in environmental space**

To test if currently realized niches (environmental space) of the three identified clades of *C. ramondioides* (mainland China, Taiwan Island and Japan) differ significantly from each other or share common climatic characteristics (i.e. niches have either diverged or are conserved), we employed the Principal Component Analysis of environmental variables (PCA-env) comparison framework (Broennimann et al., 2012; Silva et al., 2016; Herrando-Moraira et al., 2019) by using RStudio platform (2014). The same occurrences and uncorrelated and biologically significant bioclimatic

variables for SDM were inputted. The original occurrences were trimmed to guarantee a minimum distance of 5 km between them by using the "thin" function of the spThin R package (Aiello-Lammens et al., 2015), followed by a correction with a kernel smoother density function (Broennimann et al., 2012, 2014). Finally, a total of 74 input occurrences were obtained. Then we projected the smoothed densities into a global environmental space with 100 × 100 of grid-cell resolution, having each cell a sole combination of climatic conditions. The global environmental space was delimited with the background areas, based on a minimum convex polygon with a buffer size of 0.3° as Silva et al. (2016). The PCA-env plots were visualized as the individual plots for each of the three geographic regions and the global plot in which all tested niches were simultaneously represented.

The levels of niche divergence/conservatism were quantified between pairs of the defined geographic units, i.e. mainland China, Taiwan Island, and Japan, by using the Schoener's $D_S$ niche overlap metric (Schoener, 1970; Warren et al., 2008), which ranges from 0 (no overlap scenario) to 1 (completely overlap scenario).

To assess whether compared niches are more equivalent or similar than expected by chance, the niche equivalency and niche similarity tests were computed, respectively (Broennimann et al., 2012). The main difference between the two tests is that the former only considers the occurrences, while the latter also takes the surrounding areas where the pre-defined units occur into account. In the two tests, the observed $D_S$ values ($D_{obs}$) were compared to a null distribution of 100 simulated $D_S$ values ($D_{sim}$), with three possible scenarios after a two-tailed test: (1) $D_{obs} > D_{sim}$ with

$P < 0.05$, indicating niches are more equivalent or similar than randomly expected; (2) $D_{obs} < D_{sim}$ with $P < 0.05$, indicating niches are less equivalent or similar than expected by chance; (3) if $D_{obs}$ falls within 95% of $D_{sim}$ values with $P > 0.05$, the null hypothesis of niche equivalency or similarity cannot be rejected.

To infer niche conservatism (more equivalency or similarity) or niche divergence (less equivalency or similarity), both analyses were run twice in a one-tailed test with the argument "alternative" set to "lower" or "higher" in the function "ecospat.niche.similarity.test" and "ecospat.niche.equivalency.test" (R package "ecospat", Broennimann et al., 2014).

# 3 RESULTS

## 3.1 Sequence data quality and genetic diversity

A total of 108 individuals of *C. ramondioides* were sequenced using seven lanes of Illumina that produced a total of >425 million reads. Over 7 million reads passed our quality control and over 418 million reads in total were used in the assembly of the RAD-tags. After SNP filtering, we obtained 2194 RAD loci containing 16,206 SNPs that could be used for population genetic analyses.

Based on 19,668 polymorphic sites, the average percentage of genomic polymorphic sites (%*P*) for each population was 0.968 and ranged from 0.957 to 0.976 (Table 2). Private alleles were present in all populations and varied from 279 (MC-HS population) to a maximum of 1302 (JP-CB population). Observed heterozygosity ($H_O$) across populations ranged from 0.029 to 0.057 for each

284 population (average = 0.040), and expected heterozygosity ($H_E$) did from 0.042 to
285 0.062 (average = 0.050). Expected heterozygosity was consistently higher than
286 observed heterozygosity in all populations, and nucleotide diversity ($\pi$) across
287 populations ranged from 0.030 to 0.061 (average = 0.043, Table 2).

288 Based on $\pi$ and $H_E$ values, within-population genomic diversity levels were
289 generally rank-ordered per biogeographical area as JP > TW > MC (Table 2). The
290 inbreeding coefficient ($F_{IS}$) ranged from -0.024 to 0.005, indicating no inbreeding
291 within populations.

292 **3.2 Population genetic structure**

293 Pairwise $F_{ST}$ values among populations ranged from 0.136 to 0.561 (average = 0.335),
294 indicating high interpopulation differentiation. In particular, the large geographic
295 distances between populations of mainland China and Taiwan Island+Japan
296 corresponded to relatively high pairwise $F_{ST}$ values (above 0.400, except for the pair
297 TW-XZ/MC-TS with $F_{ST}$ = 0.396), suggesting high levels of population
298 differentiation between these regions. By contrast, the $F_{ST}$ values between
299 intra-mainland China populations were mostly between 0.250 and 0.350 (except $F_{ST}$ =
300 0.169 between MC-WY and MC-HS) (Table S1).

301 The ADMIXTURE software determined that the number of groups that
302 maximized the clustering of genetically similar individuals together with lowest
303 cross-validation error was $K$ = 2 (Figure 1), although $K$ = 3 was another reasonable
304 clustering model. When $K$ = 2, the 108 individuals were divided into those belonging
305 to mainland China plus Taiwan Island populations (as one class) and Japan

306 populations (as another class). When $K$ = 3, Taiwanese populations were separated
307 from those from mainland China.

308 Consistent with the $K$ = 3 clustering in ADMIXTURE, the AMOVA showed a
309 higher level of genetic differentiation among three groups (Japan, mainland China,
310 and Taiwan Island, variation = 45.91%) than among two groups (Japan vs. mainland
311 China+Taiwan, variation = 24.12%); indeed, for $K$ = 2 most variation was due to the
312 among populations within groups component (61.71%) (Table 3). The PCA (Figure 2a)
313 also revealed three distinct clusters. Similarly, the maximum likelihood phylogenetic
314 analysis grouped the 108 individuals into three robust clades (over 90% bootstrap
315 support, Figures 3, S1).

316 The Mantel test showed a significant positive correlation between pairwise
317 genetic distance and geographic distance ($r$ = 0.499, $p$ < 0.01, Figure S2), and the
318 Barrier analysis indicated that there were three major genetic boundaries (isolation
319 lines) among the studied populations (Figure 2b): line ‘a’ (which corresponds to
320 Tokyo Bay, in Japan) separated JP-CB from the rest; line ‘b’ (Taiwan Strait) separated
321 the populations from Taiwan Island and mainland China; and line ‘c’ (East China Sea)
322 separated Chinese and Japanese populations.

323 **3.3 Demographic history**

324 DIYABC estimations of the divergence history of *C. ramondioides* indicated that the
325 scenario 4 had the best fit to our data, with highest posterior probability = 0.9997,
326 95% CI = 0.9582–1.0000 (Figure 4a, Table S2), depicting the origin of both Group
327 MC and Group JP from a common uncertain ancestor (group MC+JP), and which

would have split into the two lineages at ca. 11.850 Ma (95% CI: 6.810–15.660 Ma), followed by an origin of Group TW from Group MC at ca. 4.050 Ma (95% CI: 2.601–7.410 Ma). The best fit scenario of demographic history for both Group TW and Group JP was scenario 2, and for Group MC was scenario 3 (Figure S3B). Group MC was found to experience a population contraction at ca. 1.755 Ma (95% CI: 0.690–2.613 Ma). Group TW experienced a contraction at ca. 1.653 Ma (95% CI: 0.453–2.934 Ma), followed by expansion at ca. 0.166 Ma (95% CI: 0.049–0.289 Ma), whereas the contraction and expansion of Group JP would have taken place at ca. 0.804 Ma (95% CI: 0.471–1.116 Ma) and ca. 0.193 Ma (95% CI: 0.036–0.289 Ma), respectively (Figures 4b, S3C).

### 3.4 Species distribution models

The AUC value was very high (mean ± SD = 0.971 ± 0.009; Figure S4), indicating a high predictive power by MaxEnt. The most contributing bioclimatic variables in the four time periods considered were bio19 (precipitation of coldest quarter), bio12 (annual precipitation) and bio10 (mean temperature of warmest quarter) (Table 4, Figure S5). The potential suitable areas along the different climate scenarios showed relatively large changes (Table 5); detecting both range expansions and contractions between time periods (Table 6). The predictions for the LGM based on CCSM4, MIROC and MPI-ESM-P were mostly consistent regarding total potential areas (i.e. a general range gain pattern compared to the present time; Table 5), except for moderately suitable areas that are much fewer in mainland China for the CCSM4 (Figure 5). The model showed that some area loss (ca. 20%) is expected for the year

2070 under a heavy global warming scenario (RCP 8.5; Table 5). The mountains of southeastern China, northern Taiwan Island and southwestern Japan were depicted as potential across all climate scenarios (Figure 5). If we try to translate the potential range expansions/contractions to the three detected genetic clusters, most changes corresponded to mainland China, which very considerable range contractions from LGM to future (Figure 5).

### 3.5 Niche comparisons in environment space

Based on 74 input occurrence data (Figure 6a) and nine climatic variables (bio2, bio3, bio5, bio8, bio10–12, bio16, and bio19), the results showed that the first two components of the PCA-env explained 60.76% of the total climatic variables examined, with PC1 = 32.05% and PC2 = 28.71% (Figure 6b, c). The mean diurnal range (bio2) was the most contributing variable to PC1, while bio2, isothermality (bio3) and precipitation of wettest quarter (bio16) were the variables most intensely associated with PC2. Mainland China and Japan showed very close realized niches, with that of Taiwan Island very distant from them (Figure 6b, c).

A similar pattern was detected by the niche overlap index (Scheoener's $D_S$) (Table 7); the highest $D_S$ values were found between mainland China and Japan ($D_S$ = 0.201), followed by those between Japan and Taiwan Island ($D_S$ = 0.128), and between mainland China and Taiwan Island ($D_S$ = 0). A niche divergence scenario was detected between Taiwan Island and each of the other two clades (mainland China and Japan) by the niche equivalency test (Table 7). However, the niche similarity test, which takes the surrounding areas where the clades occur into account, was not

capable to detect any signal of niche divergence (or niche conservatism) among the three clades.

# 4 DISCUSSION

Based on population genomic data, a strong population genetic structure was found for a monotypic and relict species *C. ramondioides* in the complex and highly fragmented habitats of the Sino-Japanese floristic region (SJFR, Figure 1). The patterns of phylogeographic structure detected by coalescent analyses were also congruent, and three genetic barriers were identified (Figure 2b), which captured the main characteristics of population divergence history. Coalescent methods and species distribution modeling generally support that the three genetic groups have survived in various refugia during Quaternary glacial cycles, albeit experiencing several expansions/contractions (Figures 4, 5), and formed a deep ecological niche divergences among regions (Figure 6).

## 4.1 Genetic diversity and phylogeographic pattern

The very low population-level genetic diversity of *C. ramondioides* ($H_E$: 0.042–0.062, π: 0.030–0.061) (Table 2), coincides with former studies in the species using the gene *Gcyc*1 (Xiao, 2005; Xiao et al., 2012) and suggests a combined effect of small population sizes, low success of sexual reproduction, and restricted gene flow in *C. ramondioides*. The AMOVA analysis and $F_{ST}$ values among *C. ramondioides* populations also show that most genetic variation resides among populations (40.04%)

394 and regions (45.91%), indicating little gene flow between populations and regions.
395 This herb occurs in populations of small size mostly on streamside rocks in valleys
396 under evergreen broad-leaved forests (Xiao et al., 2012); these sites are, in addition,
397 characterized by a high pollen limitation due to low levels of insect visitation (Xiao,
398 2005; Hsin & Wang, 2018; M.X. Ren, pers. observ.), although its actinomorphic
399 flowers may help to attract generalized pollinators (Wang et al., 2010; Hsin & Wang,
400 2018). The isolated nature of the habitats where *C. ramondioides* is dwelling (moist
401 rocks) is enhanced by recent human disturbance, including the tourism activities and
402 hydropower development observed in many populations (Wang, 2004; Xiao, 2005;
403 Wang et al., 2010). All these factors combined compromise successful pollination and
404 seed germination, thereby accelerating the rate of genetic erosion within populations
405 via increased inbreeding and genetic drift (Young et al., 1996; Hsin & Wang, 2018),
406 as well as promoting genetic differentiation among populations and regions (Xiao et
407 al., 2012). ADMIXTURE analysis, PCA and the phylogenetic tree all indicate that
408 there are three distinct genetic lineages within *C. ramondioides*, which correspond to
409 the three main regions where the species is present, i.e. mainland China, Taiwan
410 Island, and Japan (Figures 1, 2a, 3b). Hsin (2019), using single copy nuclear markers,
411 also identified these three genetic clusters, while Xiao et al. (2012) also found two
412 genetic clusters for China (i.e. mainland China and Taiwan Island) with
413 CYCLOIDEA1 (GCYC1) coding sequence. The clear genetic clustering pattern,
414 which has a strong geographic basis, together with significant positive correlation
415 between genetic distance and geographic distance at the population level ($r$ = 0.499, $p$

= 0.01; Figure S2), suggest that geographic isolation is the main reason for genetic differentiation within *C. ramondioides*.

Geographic barriers, such as islands, valleys and rivers, are often responsible for population differentiation and phylogeographic structure through weakening or blocking gene flow (MacArthur & Wilson, 1967; Li et al., 2011; Robin et al., 2015). Three major genetic barriers have been detected in *C. ramondioides*, which coincide with extant large topographic barriers within the species range: the East China Sea, Taiwan Strait and Tokyo Bay (Figure 2b); thus, it is possible to conclude that these landscape interruptions have played an outstanding role in the formation of phylogeographic structure of this small gesneriad and, thus, in the shaping of its three current genetic clades. Within the Japanese distribution area, one unexpected genetic boundary was found at the Tokyo Bay (Figure 3a), which is located at the "Fossa Magna", a great rift in Honshu Island caused by the collision and merging of central and northern Japan ca. 15 Ma (Kato, 1992), which would have facilitated genetic differentiation between JP-CB and JP-CCB/JP-YD. In addition to the role played by this rift, it should be noted the current Boso Peninsula (where JP-CB is situated) became an island separated from the main Honshu Island during middle Pleistocene (Shimizu & Ueshima, 2000; Kase et al., 2013), where populations JP-CCB and JP-YD occur. Therefore, the JP-CB population may have experienced further geographic isolation with respect to JP-CCB and JP-YD populations, thus accumulating distinctive genetic variation (note the much longer branch of JP-CB in the phylogeny of Figure 3). Other studies with Japanese native species also find substantial genetic

438 divergence between northern and central regions in Honshu, including plants (Senni et
439 al., 2005; Ikeda et al., 2006; Hiraoka & Tomaru, 2009; Qiu et al., 2009), insects (Sota
440 & Hayashi, 2007; Schoville et al., 2013; Saito & Tojo, 2016), and vertebrates
441 (Nunome et al., 2010; Oshida et al., 2009; Setiamarga et al., 2009).

442 **4.2 Historical demography**

443 As an East Asian endemic lineage, *Conandron* is, strangely, phylogenetically close to
444 the Southeast Asian *Ridleyandra* (Roalson & Roberts, 2016). These two genera are
445 taxonomically placed within the Didymocarpoid Gesneriaceae (Weber, 2004), one of
446 the most ancient groups in the family, whose origin lies between late Cretaceous
447 (69.66 Ma [48.20–77.06]; Roalson & Roberts, 2016) and middle Eocene (44.70 Ma
448 [37.10–60.50]; Perret et al., 2013). The crown age of *Conandron* is estimated to be ca.
449 30 Ma in late Oligocene, confirming the monotypic *Conandron* as a relict lineage in
450 East Asia.

451 The DIYABC analyses suggested that scenario 4 was the best fit model based on
452 genomic data, which showed that Group MC and Group JP originated from a
453 uncertain common ancestor (Group MC+JP, Figure 4a), and Group TW was
454 originated from Group MC. As a relict plant, the ancestral lineage of *C. ramondioides*
455 would have expanded across the whole SJFR long time ago, and became fragmented
456 much later, probably as a consequence of orogenic movements in East Asia. Firstly,
457 Japanese islands separated from continental eastern Asia during the mid-Miocene
458 opening of the Sea of Japan (22–15 Ma; Barnes, 2003; Schoville et al., 2013; Saito &
459 Tojo, 2016), which offered opportunities for population divergence of *Paris japonica*

(Yang et al., 2019), *Galium* (Jeong et al., 2016) and *Neolitsea sericea* (Lee et al., 2013). According to our results, Group MC and Group JP began to diverge at ca. 11.850 Ma (95% CI: 6.180–15.660 Ma), which suggests that the formation of the Sea of Japan would have driven genetic isolation between the two sides of the sea. Certainly, the divergence between groups MC and JP would have taken place before the first formation of the East China Sea land bridge (7.0–5.0 Ma; Kimura, 2003), which connected Japan with the continent again. Secondly, Taiwan Island was formed more recently, after orogenic movements generated by the collision of Philippine Sea Plate and the Eurasia plate at ca. 9 Ma, in late Miocene (Sibuet & Hsu, 2004). Subsequently, the orogeny of Central Range in Taiwan Island at ca. 5–6 Ma created many new habitats, thus promoting the formation of Taiwan flora in late Miocene and early Pliocene (Sibuet & Hsu, 2004). Such tectonic events would have facilitated the dispersal of *C. ramondioides* from mainland China and its establishment in Taiwan Island shortly after (ca. 4.050 Ma, 95% CI: 2.601–7.410 Ma). Therefore, both diversification events would have occurred just before the Quaternary. The same branching order was also found by Hsin (2019), although with different tempos: ca. 1.13 Ma (95% CI: 0.26–1.80 Ma) for the first diversification event between group MC and group JP, and 0.75 Ma (95% CI: 0.37–1.00 Ma) for the second diversification event between group MC and group TW; this time disparity with respect to our results may be due to the small number of mutant nucleotide sites used in the previous study of Hsin (2019).

The emergence and rapid uplift of Taiwan island, with an active orogeny that

482 resulted in the Taiwan's Central Mountain Range, made available many new niches
483 that *C. ramondioides* could explore. The niche comparison among the genetic clades
484 shows that Taiwan's one occupy a considerable different climatic space, particularly
485 regarding the occurrences (but also partly for the background; Figure 6), which may
486 indicate a progressing evolutionary niche shift and climatic speciation after dispersal
487 of *C. ramondioides* from mainland China to Taiwan Island in early Pliocene. Similarly,
488 an ecological niche divergence scenario was found between *Cypripedium*
489 *formosanum* (endemic to Taiwan Island) and its relative *C. japonicum* (widespread in
490 mainland China, Korea and Japan) (Han et al., 2022). In contrast, the strong genetic
491 differentiation between mainland Chinese and Japanese populations cannot be
492 translated to the climatic niche, probably because they share the same climatic
493 background (Figure 6).

494 It is generally acknowledged that climatic fluctuations during the Pleistocene had
495 dramatic effect on phylogeographic patterns and demographic history of plant species
496 (Comes & Kadereit, 1998; Hewitt, 2004), especially for the cold-adapted montane
497 species distributed in the SJFR that are particularly vulnerable to past climatic
498 changes (Sun et al., 2014; Xia et al., 2022). Our demographic models show that
499 Group TW, once diverged from Group MC, would have experienced a population
500 contraction at ca. 1.653 Ma (95% CI: 0.453–2.934 Ma), followed by an expansion at
501 ca. 0.166 Ma (95% CI: 0.049–0.289 Ma) (Figure 4B). Group MC experienced a large
502 population contraction at ca. 1.755 Ma (95% CI: 0.690–2.613 Ma), while Group JP
503 maintained a more or less stable population size before late Pleistocene, with the

except of a recent bottleneck from ca. 0.804 Ma (95% CI: 0.471–1.116 kyr) to ca. 0.193 Ma (95% CI: 0.036–0.289 Ma). Population contractions for TW and MC at ca. 1.7 Ma, and for JP at 0.8 Ma are not casual; rather, they may be linked to the deterioration of climate conditions at the onset of the Calabrian period and the end of the Mid-Pleistocene Transition, respectively. These climatic changes produced the decline and extirpation of several relict lineages from Europe, where very accurate pollen and plant macrofossil records are available. For example, *Taxodium* started to decline in Greece at about 1.8 Ma, while *Eucommia* disappeared from Spain and France ca. 0.8 Ma, and *Cathaya* and *Tsuga* from S Italy and N Italy, respectively, at about 0.75 Ma (Magri et al., 2017).

Differently to that occurred in Europe and also in N America, where the late Neogene much harsher climatic conditions did not allow most thermophilic elements to survive (Latham and Ricklefs, 1993; Manchester et al., 2009), the large and rather continuous mountain systems in East China (including Taiwan) and Japan offered extensive stable but fragmented habitats, likely serving as long-term stable refugia for *C. ramondioides* and other East Asia relict plant in the humid subtropical/warm-temperate areas (López-Pujol et al., 2011; Tang et al., 2018). Even at the LGM, large areas would have been suitable for *C. ramondioides* (Fig, 5).

### 4.3 Dispersal vs. vicariance in East Asia

Our genetic data of *C. ramondioides* indicates a strong phylogeographic structure consisting of three genetic clusters that have a strong geographical basis (Figures 1, 2). After Japanese islands separated from continental eastern Asia during the

mid-Miocene, the East China Sea land bridge re-connected mainland China and Japan during several periods (7.0–5.0 Ma; 2.0–1.3 Ma, and the glacial cycles during the period 0.2–0.015 Ma; Kimura, 2003). The frequent connection provided by the land bridge offered opportunities to the dispersal of plants (Chung et al., 2007; Qi et al., 2012; Sakaguchi et al., 2012; Jiang et al., 2021), but this not always offered suitable habitats (i.e., acting as a "filter"; Qiu et al., 2011; Qi et al., 2014). For *C. ramondioides*, the East China Sea land bridge would not have enabled enough gene flow to prevent the strong divergence detected in the present study, which could be due to the lack of suitable habitats throughout most of the land bridge in the glacial periods (Figure 5).

The Taiwan flora may have its origin in mainland China, Ryukyu Islands and tropical Asian regions (Philippines or Vietnam) during late Miocene and early Pliocene (Hsieh, 2003; Chiang & Schaal, 2006). Our demographic models show that the Taiwanese populations of *C. ramondioides* likely originated from Group MC instead of Group JP (at ca. 4.050 Ma), in agreement with other plants of the SJFR (e.g. *Paris japonica*; Yang et al., 2019), but contrary to other examples such as *Trochodendron aralioides* (which dispersed from Japan to Taiwan Island throughout Ryukyu Islands; Huang et al., 2004). Besides, formed by the uplift of Taiwan since the Pliocene (Yu & Chou, 2001; Yu, 2003), Taiwan Strait has acted as a primary genetic barrier between the mainland and the island in many plants (Ruan et al., 2013; Ge et al., 2015), including relict ones (Chou et al., 2011; Qiu et al., 2017). This seems to be also the case of *C. ramondioides*, in spite of most of the Taiwan Strait would have

548 been passable at during the cold periods of the Quaternary (since 2 Ma, marine
549 regressions at glacial maxima reached at least –70 m; Miller et al., 2005).
550

551 ## 5 Conclusions

552 This is the first time that the Tertiary relict plant *Conandron ramondioides*, distributed
553 in mainland China, Taiwan Island and Japan, was used to as a case study to shed light
554 on the relative roles of dispersal vs. vicariance processes in Sino-Japanese plant
555 disjunctions. The reconstruction of the phylogeographical relationships and
556 population history within *C. ramondioides*, alongside with the species distribution
557 models, highlight that the predominance of vicariance processes to explain the current
558 distribution of this relict plant, with three distinct genetic lineages corresponding to
559 three well-defined different geographical regions. The sharp genetic differentiation
560 among the three clusters of *C. ramondioides* would be due to low levels of historical
561 gene flow, associated with a long history of geographical isolation before the
562 Quaternary. Our results indicate that RAD-seq methods can be used successfully to
563 examine patterns of historical phylogeography and to assess the relative roles of
564 dispersal and vicariance in species disjunctions. We suggest, nevertheless, that a
565 taxonomic survey with more extensive sampling and detailed morphological
566 comparisons is needed in order to assess whether the three distinct geographically and
567 genetically isolated lineages might represent three subspecies or even cryptic species
568 by constituting *C. ramondioides* complex. Indeed, two varieties based on
569 morphological characters have been recognized: var. *ramondioides* and var.

570 *taiwanensis* based on studied plants from Japan and Taiwan, respectively
571 (Kokubugata & Peng, 2004). The seemingly diverging niche of the Taiwanese clade
572 with respect to that of Japan (and mainland China) clade(s) are supporting this
573 distinction.
574

575 ## ACKNOWLEDGEMENTS

576 We thank Xiang-Wen Hou and Zi-Yun Ren for assistance in fieldwork and Xuan Jin
577 and Yuan-Mi Wu for assistance in data analysis. Financial support was provided by
578 National Natural Science Foundation of China (41871041).
579

580 ## AUTHOR CONTRIBUTIONS

581 Ming-Xun Ren applied for funding, organized sampling and designed the study.
582 Ming-Xun Ren and Ke Tan conceived the study. Ke Tan contributed in the
583 demographic analyses. Xiao-Lan Yao contributed in the climatic niche difference
584 analyses. Shao-Jun Ling led the bioinformatics and statistical analysis, prepared
585 figures, and wrote the draft with contributions from Ming-Xun Ren, Jordi
586 López-Pujol and Juli Caujapé-Castells.

587 ## CONFLICT OF INTEREST

588 There is no conflict of interest.
589

590 ## DATA AVAILABILITY STATEMENT

591 The demultiplexed fastq data are archived in NCBI SRA (BioProject ID:

PRJNA821665).

## ORCID

*Shao-Jun Ling* https://orcid.org/0000-0002-4675-8250

*Xiao-Lan Yao* https://orcid.org/0000-0002-5908-0979

*Juli Caujapé-Castells* https://orcid.org/0000-0003-0600-1496

*Jordi López-Pujol* https://orcid.org/0000-0002-2091-6222

*Ke Tan* https://orcid.org/0000-0002-9036-163X

*Ming-Xun Ren* https://orcid.org/0000-0002-4707-2656

## REFERENCES

Alexander, D. H., Novembre, J., & Lange, K. (2009). Fast model-based estimation of ancestry in unrelated individuals. *Genome Research*, *19(9)*, 1655–1664. https://doi.org/10.1101/gr.094052.109

Aiello-Lammens, M. E., Boria, R. A., Radosavljevic, A., Vilela, B., & Anderson, R. P. (2015). spThin: an R package for spatial thinning of species occurrence records for use in ecological niche models. *Ecography*, *38(5)*, 541–545. https://doi.org/10.1111/ecog.01132

Barnes, G. L. (2003). Origins of the Japanese Islands: The New “Big Picture”. *Japan Review*, *15*, 3–50. https://www.jstor.org/stable/25791268

Baldwin, R. A. (2009). Use of maximum entropy modeling in wildlife research. *Entropy*, *11(4)*, 854–866. https://doi.org/10.3390/e11040854

Broennimann, O., Fitzpatrick, M. C., Pearman, P. B., Petitpierre, B., Pellissier, L., Yoccoz, N. G., Thuiller, W., Fortin, M. J., Randin, C., Zimmermann, N. E., Graham, C. H., & Guisan, A. (2012). Measuring ecological niche overlap from occurrence and spatial environmental data. *Global Ecology and Biogeography*, *21(4)*, 481–497. https://doi.org/10.1111/j.1466-8238.2011.00698.x

Broennimann, O., Di Cola, V., Petitpierre, B., Breiner, F., Scherrer, D., D’ Amen, M., Randin, C., Engler, R., Hordijk, W., Mod, H., Pottier, J., Di Febbraro, M., Pellissier, L., Pio, D., Mateo, R. G., Dubuis, A., Maiorano, L., Psomas, A., Ndiribe, C., Salamin, N., Zimmermann, N., & Guisan, A. (2014). Ecospat: Spatial ecology miscellaneous methods. R package version 1.0. Department of Ecology and Evolution (DEE) and Institute of Earth Surface Dynamics (IDYST), University of Lausanne, Switzerland.

626 http://CRAN.R-project.org/package=ecospat (accessed 2 May 2020).
627 Catchen, J., Hohenlohe, P. A., Bassham, S., Amores, A., & Cresko, W. A. (2013).
628 Stacks: an analysis tool set for population genomics. *Molecular Ecology*, *22(11)*,
629 3124–3140. https://doi.org/10.1111/mec.12354
630 Caujapé-Castells, J., García-Verdugo, C., Marrero-Rodríguez, Á., Fernández-Palacios,
631 J. M., Crawford, D. J., & Mort, M. E. (2017). Island ontogenies, syngameons,
632 and the origins and evolution of genetic diversity in the Canarian endemic flora.
633 *Perspectives in Plant Ecology, Ecology and Systematics*, *27*, 9–22.
634 https://doi.org/10.1016/j.ppees.2017.03.003
635 Chiang, Y. C., & Schaal, B. A. (2006). Phylogeography of plants in Taiwan and the
636 Ryukyu Archipelago. *Taxon*, *55(1)*, 31–41. https://doi.org/10.2307/25065526
637 Chung, C. H. (2007). Vegetation response to climate change on Jeju Island, South
638 Korea, during the last deglaciation based on pollen record. *Geosciences Journal*,
639 *11(2)*, 147–155. https://doi.org/10.1007/BF02913928
640 Chou, Y. W., Thomas, P. I., Ge, X. J., LePage, B. A., & Wang, C. N. (2011). Refugia
641 and phylogeography of *Taiwania* in East Asia. *Journal of Biogeography*, *38(10)*,
642 1992–2005. https://doi.org/10.1111/j.1365-2699.2011.02537.x
643 Collins, M., Knutti, R., Arblaster, J., Dufresne, J. L., Fichefet, T., Friedlingstein, P.,
644 Gao, X., Gutowski, W. J., Johns, T., Krinner, G., Shongwe, M., Tebaldi, C.,
645 Weaver, A. J., Wehner, M. F., Allen, M. R., Andrews, T., Beyerle, U., Bitz, C. M.,
646 Bony, S., & Booth, B. B. B. (2013). Long-term climate change: Projections,
647 commitments and irreversibility. In T. F. Stocker, D. Qin, G. K. Plattner, M.
648 Tignor, S. K. Allen, J. Doschung, A. Nauels, Y. Xia, V. Bex, & P. M. Midgley
649 (Eds), *Climate change 2013: The physical science basis. Contribution of working*
650 *group I to the fifth assessment report of the intergovernmental panel on climate*
651 *change* (pp. 1029–1136). Cambridge University Press.
652 https://doi.org/10.1017/CBO9781107415324.024
653 Comes, H. P., & Kadereit, J. W. (1998). The effect of Quaternary climatic changes on
654 plant distribution and evolution. *Trends in Plant Science*, *3(11)*, 432–438.
655 https://doi.org/10.1016/S1360-1385(98)01327-2
656 Cornuet, J. M., Ravigné, V., & Estoup, A. (2010). Inference on population history and
657 model checking using DNA sequence and microsatellite data with the software
658 DIYABC (v1.0). *BMC Bioinformatics*, *11*, 401.
659 https://doi.org/10.1186/1471-2105-11-401
660 Cornuet, J. M., Pudlo, P., Veyssier, J., Dehne-Garcia, A., Gautier, M., Leblois, R.,
661 Marin, J. M., & Estoup, A. (2014). DIYABC v2.0: a software to make
662 Approximate Bayesian Computation inferences about population history using
663 Single Nucleotide Polymorphism, DNA sequence and microsatellite data.
664 *Bioinformatics*, *30(8)*, 1187–1189. https://doi.org/10.1093/bioinformatics/btt763
665 Danecek, P., Auton, A., Abecasis, G., Albers, C. A., Banks, E., DePristo, M. A.,
666 Handsaker, R. E., Lunter, G., Marth, G. T., Sherry, S. T., McVean, G., & Durbin,
667 R. (2011). The variant call format and VCFtools. *Bioinformatics*, *27(15)*,
668 2156–2158. https://doi.org/10.1093/bioinformatics/btr330
669 Decker, J. E., McKay, S. D., Rolf, M. M., Kim, J., Alcalá, A. M., Sonstegard, T. S.,

Hanotte, O., Götherström, A., Seabury, C. M., Praharani, L., Babar, M. E., de Almeida Regitano, L. C., Yildiz, M. A., Heaton, M. P., Liu, W. S., Lei, C. Z., Reecy, J. M., Saif-Ur-Rehman, M., Schnabel, R. D., & Taylor, J. F. (2014). Worldwide patterns of ancestry, divergence, and admixture in domesticated cattle. *PLoS Genetics*, *10(3)*, e1004254. https://doi.org/10.1371/journal.pgen.1004254

Doyle, J. J., & Doyle, J. L. (1987). A rapid DNA isolation procedure for small quantities of fresh leaf tissues. *Phytochemical Bulletin*, *19(1)*, 11–15. https://doi.org/10.1016/0031-9422(80)85004-7

Excoffier, L., & Lischer, H. E. (2010). Arlequin suite ver 3.5: a new series of programs to perform population genetics analyses under Linux and Windows. *Molecular Ecology Resources*, *10(3)*, 564–567. https://doi.org/10.1111/j.1755-0998.2010.02847.x

Fielding, A. H., & Bell, J. F. (1997). A review of methods for the assessment of prediction errors in conservation presence/absence models. *Environmental Conservation*, *24(1)*, 38–49. https://doi.org/10.1017/S0376892997000088

Ge, X. J., Hung, K. H., Ko, Y. Z., Hsu, T. W., Gong, X., Chiang, T. Y., & Chiang, Y. C. (2015). Genetic divergence and biogeographical patterns in *Amentotaxus argotaenia* specise complex. *Plant Molecular Biology Reporter*, *33*, 264–280. https://doi.org/10.1007/s11105-014-0742-0

Gent, P. R., Danabasoglu, G., Donner, L. J., Holland, M. M., Hunke, E. C., Jayne, S. R., Lawrence, D. M., Neale, R. B., Rasch, P. J., Vertenstein, M., Worley, P. H., Yang, Z. L., & Zhang, M. H. (2011). The community climate system model version 4. *Journal of Climate*, *24(19)*, 4973–4991. https://doi.org/10.1175/2011JCLI4083.1

Han, L. X., Jin, Y., Zhang J. L., Li, X. L., Chung, M. Y., Herrando-Moraira, S., Kawahara, T., Yukawa, T., Chung, S.-W., Chung, J. M., Kim, Y. D., López-Pujol, J., Chung, M. G. & Tian, H. Z. 2022. Phylogeography of the endangered orchids *Cypripedium japonicum* and *Cypripedium formosanum* in East Asia: Deep divergence at infra- and interspecific levels. *Taxon*, published online, https://doi.org/10.1002/tax.12710

Hewitt, G. M. (2004). Genetic consequences of climatic oscillations in the Quaternary. *Philosophical Transactions of the Royal Society B: Biological Sciences*, *359(1442)*, 183–195. https://doi.org/10.1098/rstb.2003.1388

Herrando-Moraira, S., Nualart, N., Herrando-Moraira, A., Chung, M. Y., Chung, M. G., & López-Pujol, J. (2019). Climatic niche characteristics of native and invasive *Lilium lancifolium*. *Scientific Reports*, *9(1)*, 14334. https://doi.org/10.1038/s41598-019-50762-4

Hijmans, R. J., Cameron, S. E., Parra, J. L., Jones, P. G., & Jarvis, A. (2005). Very high resolution interpolated climate surfaces for global land areas. *International Journal of Climatology*, *25(15)*, 1965–1978. https://doi.org/10.1002/joc.1276

Hiraoka, K., & Tomaru, N. (2009). Genetic divergence in nuclear genomes between populations of *Fagus crenata* along the Japan Sea and Pacific sides of Japan. *Journal of Plant Research*, *122(3)*, 269–282.

https://doi.org/10.1007/s10265-009-0217-9
Hsieh, C. F. (2003). Composition, endemism and phytogeographical affinities of the Taiwan flora. In Editorial Committee of the Flora of Taiwan (Eds.) *Flora of Taiwan* (2nd ed., pp. 1–14). Department of Botany, National Taiwan University, Taipei.
Hsin, K. T. (2019). *Phylogeography, flower development and selection on floral symmetry gene in East Asia endemic Conandron ramondioides*. National Taiwan University, PhD Dissertation, Taipei. http://tdr.lib.ntu.edu.tw/jspui/handle/123456789/78785
Hsin, K. T., & Wang, C. N. (2018). Expression shifts of floral symmetry genes correlate to flower actinomorphy in East Asia endemic *Conandron ramondioides* (Gesneriaceae). *Botanical Studies*, *59(1)*, 24. https://doi.org/10.1186/s40529-018-0242-x
Hu, C. M., & Kelso, S. (1996). *Flora of China* (pp. 15, 99–185). Beijing: Science Press.
Hudson, R. R. (2002). Generating samples under a Wright-Fisher neutral model of genetic variation. *Bioinformatics*, *18(2)*, 337–338. https://doi.org/10.1093/bioinformatics/18.2.337
Huang, S. F., Hwang, S. Y., Wang, J. C., & Lin, T. P. (2004). Phylogeography of *Trochodendron aralioides* (Trochodendraceae) in Taiwan and its adjacent areas. *Journal of Biogeography*, *31(8)*, 1251–1259. https://doi.org/10.1111/j.1365-2699.2004.01082.x
Ikeda, H., Senni, K., Fujii, N., & Setoguchi, H. (2006). Refugia of *Potentilla matsumurae* (Rosaceae) located at high mountains in the Japanese archipelago. *Molecular Ecology*, *15(12)*, 3731–3740. https://doi.org/10.1111/j.1365-294X.2006.03054.x
Iwatsuki, K., Yamazaki, T., Boufford, D. E., & Ohba, H. (1993). *Flora of Japan* (3a, pp. 376–380). Kodansha Ltd.
Jeong, K. S., Shin, J. K., Maki, M., & Pak, J. H. (2016) Phylogeny of *Galium* L. (Rubiaceae) from Korea and Japan based on chloroplast DNA sequence. *Bangladesh Journal of Plant Taxonomy*, *23(2)*, 237–246. https://doi.org/10.3329/bjpt.v23i2.30858
Jiang, K., Tong, X., Ding, Y. Q., Wang, Z. W., Miao, L. Y., Xiao, Y. E., Huang, W. C., Hong, Y. H., & Chen, X. Y. (2021). Shifting roles of the East China Sea in the phylogeography of red nanmu in East Asia. *Journal of Biogeography*, *48(10)*, 2486–2501. https://doi.org/10.1111/jbi.14215
Jombart, T. (2008). Adegenet: a R package for the multivariate analysis of genetic markers. *Bioinformatics*, *24(11)*, 1403–1405. https://doi.org/10.1093/bioinformatics/btn129
Kato, H. (1992). Fossa Magna-A masked border region separating southwest and northeast Japan. *Bulletin of the Geological Survey of Japan*, *43(1/2)*, 1–30. https://www.gsj.jp/data/bull-gsj/43-0102_02
Kase, T., Nakano, T., Kurihara, Y., & Haga, T. (2013). A middle Pleistocene limpet assemblage from central Japan (Gastropoda: Patellogastropoda) and selective

758 extinction of intertidal rocky shore molluscs in response to glacio-eustatic
759 sea-level changes. *Paleontological Research*, *17(3)*, 261–281.
760 https://doi.org/10.2517/1342-8144-17.3.261
761 Kimura, M. (2003). Land connections between Eurasian continent and Japanese
762 Islands–related to human migration. *Migration & Diffusion*, *4(13)*, 14–33.
763 Retrieved from
764 https://www.migration-diffusion.info/article.php?year=2003&id=135
765 Kokubugata, G., & Peng, C. I. (2004). Floral morphology and recognition of varieties
766 in *Conandron ramondioides* (Gesneriaceae) from Japan and Taiwan. *Edinburgh*
767 *Journal of Botany*, *61(1)*, 21–30. https://doi.org/10.1017/S0960428604000034
768 Latham, R.E., & Ricklefs, R.E. (1993). Continental comparisons of temperate-zone
769 tree species diversity. In: R. E. Ricklefs, D. Schluter (Eds.), *Species diversity in*
770 *ecological communities* (pp. 294–314). University Chicago Press.
771 Lee, J. H., Lee, D. H., & Choi, B. H. (2013). Phylogeography and genetic diversity of
772 East Asian *Neolitsea sericea* (Lauraceae) based on variations in chloroplast DNA
773 sequences. *Journal of Plant Research*, *126(2)*, 193–202.
774 https://doi.org/10.1007/s10265-012-0519-1
775 Li, Y., Zhai, S. N., Qiu, Y. X., Guo, Y. P., Ge, X. J., & Comes, H. P. (2011). Glacial
776 survival east and west of the 'Mekong–Salween Divide' in the
777 Himalaya–Hengduan Mountains region as revealed by AFLPs and cpDNA
778 sequence variation in *Sinopodophyllum hexandrum* (Berberidaceae). *Molecular*
779 *Phylogenetics and Evolution*, *59(2)*, 412–424.
780 https://doi.org/10.1016/j.ympev.2011.01.009
781 Lischer, H. E. L., & Excoffier, L. (2012). PGDSpider: An automated data conversion
782 tool for connecting population genetics and genomics programs. *Bioinformatics*,
783 *28(2)*, 298–299. https://doi.org/10.1093/bioinformatics/btr642
784 López-Pujol, J., Zhang, F. M., Sun, H. Q., Ying, T. S., & Ge, S. (2011). Centres of
785 plant endemism in China: places for survival or for speciation? *Journal of*
786 *Biogeography*, *38(7)*, 1267–1280.
787 https://doi.org/10.1111/j.1365-2699.2011.02504.x
788 MacArthur, R. H., & Wilson, E. O. (1967). *The Theory of Island Biogeography*.
789 Princeton University Press.
790 Magri, D., Di Rita, F., Aranbarri, J., Fletcher, W. & González-Sampériz, P. 2017.
791 Quaternary disappearance of tree taxa from Southern Europe: Timing and trends.
792 *Quaternary Science Reviews*, *163(1)*, 23–55.
793 https://doi.org/10.1016/j.quascirev.2017.02.014
794 Manchester, S. R., Chen, Z. D., Lu, A. M., & Uemura, K. (2009). Eastern Asian
795 endemic seed plant genera and their paleogeographic history throughout the
796 Northern Hemisphere. *Journal of Systematics and Evolution*, *47(1)*, 1–42.
797 https://doi.org/10.1111/j.1759-6831.2009.00001.x
798 Manni, F., Guerard, E., & Heyer, E. (2004). Geographic patterns of (genetic,
799 morphologic, linguistic) variation: how barriers can be detected by using
800 Monmonier's algorithm. *Human Biology*, *76(2)*, 173–190.
801 https://doi.org/10.1353/hub.2004.0034

Miller, K. G., Kominz, M. A., Browning, J. V., Wright, J. D., Mountain, G. S., Katz, M. E., Sugarman, P. J., Cramer, B. S., Christie-Blick, N., & Pekar, S. F. (2005). The Phanerozoic record of global sea-level change. *Science*, *310(5752)*, 1293–1298. https://doi. org/10.1126/science.1116412

Monmonier, M. (1973). Maximum-difference barriers: An alternative numerical regionlization method. *Geographical Analysis*, *5(3)*, 245–261. https://doi.org/10.1111/j.1538-4632.1973.tb01011.x

Nunome, M., Torii, H., Matsuki, R., Kinoshita, G., & Suzuki, H. (2010). The influence of Pleistocene refugia on the evolutionary history of the Japanese hare, Lepus brachyurus. *Zoological science*, *27(9)*, 746–754. https://doi.org/10.2108/zsj.27.746

Oshida, T., Masuda, R., & Ikeda, K. (2009). Phylogeography of the Japanese giant flying squirrel, *Petaurista leucogenys* (Rodentia: Sciuridae): implication of glacial refugia in an arboreal small mammal in the Japanese Islands. *Biological Journal of the Linnean Society*, *98(1)*, 47–60. https://doi.org/10.1111/j.1095-8312.2009.01276.x

Otto-Bliesner, B. L., Marshall, S. J., Overpeck, J. T., Miller, G. H., & Hu, A. X. (2006). Simulating Arctic climate warmth and icefield retreat in the Last Interglaciation. *Science*, *311(5768)*, 1751–1753. https://doi.org/10.1126/science.1120808

Perret, M., Chautems, A., de Araujo, A. O., & Salamin, N. (2013). Temporal and spatial origin of Gesneriaceae in the New World inferred from plastid DNA sequences. *Biological Journal of the Linnean Society, 171(1)*, 61–79. https://doi.org/10.1111/j.1095-8339.2012.01303.x

Phillips, S. J., Anderson, R. P., & Schapire, R. E. (2006). Maximum entropy modeling of species geographic distributions. *Ecological Modelling*, *190(3–4)*, 231–259. https://doi.org/10.1016/j.ecolmodel.2005.03.026

Qi, X. S., Chen, C., Comes, H. P., Sakaguchi, S., Liu, Y. H., Tanaka, N., Sakio, H., & Qiu, Y. X. (2012). Molecular data and ecological niche modelling reveal a highly dynamic evolutionary history of the East Asian Tertiary relict *Cercidiphyllum* (Cercidiphyllaceae). *New Phytologist*, *196(2)*, 617–630. https://doi.org/10.1111/j.1469-8137.2012.04242.x

Qi, X. S., Yuan, N., Comes, H. P., Sakaguchi, S., & Qiu, Y. X. (2014). A strong "filter" effect of the East China Sea land bridge for East Asia's temperate plant species: Inferences from molecular phylogeography and ecological niche modelling of *Platycrater arguta* (Hydrangeaceae). *BMC Evolutionary Biology*, *14*, 41. https://doi.org/10.1186/1471-2148-14-41

Qiu, Y. X., Fu, C. X., & Comes, H. P. (2011). Plant molecular phylogeography in China and adjacent regions: Tracing the genetic imprints of Quaternary climate and environmental change in the world's most diverse temperate flora. *Molecular Phylogenetics and Evolution*, *59(1)*, 225–244. https://doi.org/10.1016/j.ympev.2011.01.012

Qiu, Y. X., Lu, Q. X., Zhang, Y. H., & Cao, Y. N. (2017). Phylogeography of East Asia's Tertiary relict plants: current progress and future prospects. *Biodiversity*

*Science*, *25(2)*, 136–146. https://doi.org/10.17520/biods.2016292
Qiu, Y. X., Qi, X. S., Jin, X. F., Tao, X. Y., Fu, C. X., Naiki, A., & Comes, H. P. (2009). Population genetic structure, phylogeography, and demographic history of *Platycrater arguta* (Hydrangeaceae) endemic to east China and south Japan, inferred from chloroplast DNA sequence variation. *Taxon*, *58(4)*, 1226–1241. https://doi.org/10.1002/tax.584014
Robin, V. V., Vishnudas, C. K., Gupta, P., & Ramakrishnan, U. (2015). Deep and wide valleys drive nested phylogeographic patterns across a montane bird community. *Proceedings of the Royal Society B: Biological Sciences*, *282(1810)*, 20150861. https://doi.org/10.1098/rspb.2015.0861
Roalson, E. H., & Roberts, W. R. (2016). Distinct processes drive diversification in different clades of Gesneriaceae. *Systematic Biology*, *65(4)*, 662–684. https://doi.org/10.1093/sysbio/syw012
R Studio Team. (2014). *R Studio: integrated development environment for R (version 0.98.932)*. Boston, MA.
Ruan, Y., Huang, B. H., Lai, S. J., Wan, Y. T., Li, J. Q., Huang, S., & Liao, P. C. (2013). Population genetic structure, local adaptation, and conservation genetics of *Kandelia obovata*. *Tree Genetics & Genomes*, *9*, 913–925. https://doi.org/10.1007/s11295-013-0605-0
Schoener, T. W. (1970). Nonsynchronous spatial overlap of lizards in patchy habitats. *Ecology*, *51(3)*, 408–418. https://doi.org/10.2307/1935376
Silva, D. P., Vilela, B., Buzatto, B. A., Moczek, A. P., & Hortal, J. (2016). Contextualized niche shifts upon independent invasions by the dung beetle *Onthophagus taurus*. *Biological Invasions*, *18(11)*, 3137–3148. https://doi.org/10.1007/s10530-016-1204-4
Swets, J. A. (1988). Measuring the accuracy of diagnostic systems. *Science*, *240(4857)*, 1285–1293. https://doi.org/10.1126/science.3287615
Saito, R., & Tojo, K. (2016). Complex geographic-and habitat-based niche partitioning of an East Asian habitat generalist mayfly *Isonychia japonica* (Ephemeroptera: Isonychiidae) with reference to differences in genetic structure. *Freshwater Science*, *35(2)*, 712–723. https://doi.org/10.1086/686564
Sakaguchi, S., Qiu, Y. X., Liu, Y. H., Qi, X. S., Kim, S. H., Han, J. Y., Takeuchi, Y., Worth, J. R. P., Yamasaki, M., Sakurai, S., & Isagi, Y. J. (2012). Climate oscillation during the Quaternary associated with landscape heterogeneity promoted allopatric lineage divergence of a temperate tree *Kalopanax septemlobus* (Araliaceae) in East Asia. *Molecular Ecology*, *21(15)*, 3823–3838. https://doi.org/10.1111/j.1365-294X.2012.05652.x
Schoville, S. D., Uchifune, T., & Machida, R. (2013). Colliding fragment islands transport independent lineages of endemic rock-crawlers (Grylloblattodea: Grylloblattidae) in the Japanese archipelago. *Molecular Phylogenetics and Evolution*, *66(3)*, 915–927. https://doi.org/10.1016/j.ympev.2012.11.022
Senni, K., Fujii, N., Takahashi, H., Sugawara, T., & Wakabayashi, M. (2005). Intraspecific chloroplast DNA variations of the alpine plants in Japan. *Acta phytotaxonomica et Geobotanica*, *56(3)*, 265–275.

https://doi.org/10.1016/j.ympev.2012.11.022
Setiamarga, D. H. E., Miya, M., Yamanoue, Y., Azuma, Y., Inoue, J. G., Ishiguro, N. B., Mabuchi, K., & Nishida, M. (2009). Divergence time of the two regional medaka populations in Japan as a new time scale for comparative genomics of vertebrates. *Biology Letters*, *5(6)*, 812–816. https://doi.org/10.1098/rsbl.2009.0419
Shimizu, Y., & Ueshima, R. (2000). Historical biogeography and interspecific mtDNA introgression in *Euhadra peliomphala* (the Japanese land snail). *Heredity*, *85*, 84–96. https://doi.org/10.1046/j.1365-2540.2000.00730.x
Sibuet, J. C., & Hsu, S. K. (2004). How was Taiwan created? *Tectonophysics*, *379(1–4)*, 159–181. https://doi.org/10.1016/j.tecto.2003.10.022
Sota, T., & Hayashi, M. (2007). Comparative historical biogeography of *Plateumaris* leaf beetles (Coleoptera: Chrysomelidae) in Japan: interplay between fossil and molecular data. *Journal of Biogeography*, *34(6)*, 977–993. https://doi.org/10.1111/j.1365-2699.2006.01672.x
Stamatakis, A. (2006). RAxML–VI–HPC: Maximum likelihood–based phylogenetic analyses with thousands of taxa and mixed models. *Bioinformatics*, *22(21)*, 2688–2690. https://doi.org/10.1093/bioinformatics/btl446
Sun, Y. X., Moore, M. J., Yue, L. L., Feng, T., Chu, H. J., Chen, S. T., Ji, Y. H., Wang, H. C., & Li, J. Q. (2014). Chloroplast phylogeography of the East Asian Arcto-Tertiary relict *Tetracentron sinense* (Trochodendraceae). *Journal of Biogeography*, *41(9)*, 1721–1732. https://doi.org/10.1111/jbi.12323
Tallis, J. H. (1991). *Plant community history: long-term changes in plant distribution and diversity*. Chapman and Hall, London.
Tang, C. Q., Matsui, T., Ohashi, H., Dong, Y. F., Momohara, A., Herrando-Moraira, A., Qian, S. H., Yang, Y. C., Ohsawa, M., Luu, H. T., Grote, P. J., Krestov, P. V., LePage, B., Werger, M., Robertson, K., Hobohm, C., Wang, C. Y., Peng, M. C., Chen, X., Wang, H. C., Su, W. H., Zhou, R., Li, S. F., He, L. Y., Yan, K., Zhu, M. Y., Hu, J., Yang, R. H., Li, W. J., Tomita, M., Wu, Z. L., Yan, H. Z., Zhang, G. F., He, H., Yi, S. R., Gong, H., Song, K., Song, D., Li, X. S., Zhang, Z. Y., Han, P. B., Shen, L. Q., Huang, D. S., Luo, K., & López-Pujol, J. (2018). Identifying long-term stable refugia for relict plant species in East Asia. *Nature Communications*, *9(1)*, 4488. https://doi.org/10.1038/s41467-018-06837-3
Wang, Y. S., Xie, B. Y., Wan, F. H., Xiao, Q. M., & Dai, L. Y. (2007). Application of ROC curve analysis in evaluating the performance of alien species' potential distribution models. *Biodiversity Science*, *15(4)*, 365–372. https://doi.org/10.1360/biodiv.060280
Wang, Y. Z., Liang, R. H., Wang, B. H., Li, J. M., Qiu, Z. J., Li, Z. Y., & Weber, A. (2010). Origin and phylogenetic relationships of the Old World Gesneriaceae with actinomorphic flowers, inferred from ITS and *trn*L-*trn*F sequences. *Taxon*, *59(4)*, 1044–1052. https://www.jstor.org/stable/20773975
Wang, Y. Z. (2004). Conandron. In: Z. Y. Li, & Y. Z. Wang (Eds.) *Plants of Gesneriaceae in China* (pp. 3–7). Henan Science and Technology Publishing House.

Warren, D. L., Glor, R. E., & Turelli, M. (2008). Environmental niche equivalency versus conservatism: quantitative approaches to niche evolution. *Evolution*, *62(11)*, 2868–2883. https://doi.org/10.1111/j.1558-5646.2008.00482.x

Watanabe, S., Hajima, T., Sudo, K., Nagashima, T., Takemura, T., Okajima, H., Nozawa, T., Kawase, H., Abe, M., Yokohata, T., Ise, T., Sato, H., Kato, E., Takata, K., Emori, S., & Kawamiya, M. (2011). MIROC-ESM: model description and basic results of CMIP5-20c3m experiments. *Geoscientific Model Development Discussions*, *4*, 1063–1128. https://doi.org/10.5194/gmdd-4-1063-2011

Weber, A. (2004). Gesneriaceae. In: K. Kubitzki, & J. Kadereit (Eds.), *The families and genera of vascular plants* (vol. 7, pp. 63–158). Springer.

Xiao, L. H., Li, Z., Wang, R., & Wang, Y. Z. (2012). Population differentiation and phylogeographic pattern of a relict species, *Conandron ramondioides* (Gesneriaceae), revealed from sequence polymorphism and haplotypes of the *CYCLOIDEA* gene. *Journal of Systematics and Evolution*, *50(1)*, 45–57. https://doi.org/10.1111/j.1759-6831.2011.00166.x

Xiao, L. H. (2005). *Studies on molecular ecology and evolution of Conandron ramondioides (Gesneriaceae) populations*. Inner Mongolia University, Master dissertation, Hohhot.

Xia, X. M., Yang, M. Q., Li, C. L., Huang, S. X., Jin, W. T., Shen, T. T., Wang, F., Li, X. H., Yoichi, W., Zhang, L. H., Zheng, Y. R., & Wang, X. Q. (2022). Spatiotemporal Evolution of the Global Species Diversity of *Rhododendron*. *Molecular Biology and Evolution*, *39(1)*, msab314. https://doi.org/10.1093/molbev/msab314

Yang, L. F., Yang, Z. Y., Liu, C. K., He, Z. S., Zhang, Z. R., Yang, J., Liu, H. Y., Yang, J. B., & Ji, Y. H. (2019). Chloroplast phylogenomic analysis provides insights into the evolution of the largest eukaryotic genome holder, *Paris japonica* (Melanthiaceae). *BMC Plant Biology*, *19(1)*, 293. https://doi.org/10.1186/s12870-019-1879-7

Young, A., Boyle, T., & Brown, T. (1996). The population genetic consequences of habitat fragmentation for plants. *Trends in Ecology and Evolution*, *11(10)*, 413–418. https://doi.org/10.1016/0169-5347(96)10045-8

Yu, H. S., & Chou, Y. W. (2001). Physiographic and geological characteristics of shelves in north and west of Taiwan. *Science in China (Series D)*, *44(8)*, 696–707. https://doi.org/10.1007/BF02907199

Yu, H. S. (2003). Geological characteristics and distribution of submarine physiographic features in the Taiwan region. *Marine Georesources & Geotechnology*, *21(3–4)*, 139–153. https://doi.org/10.1080/713773391

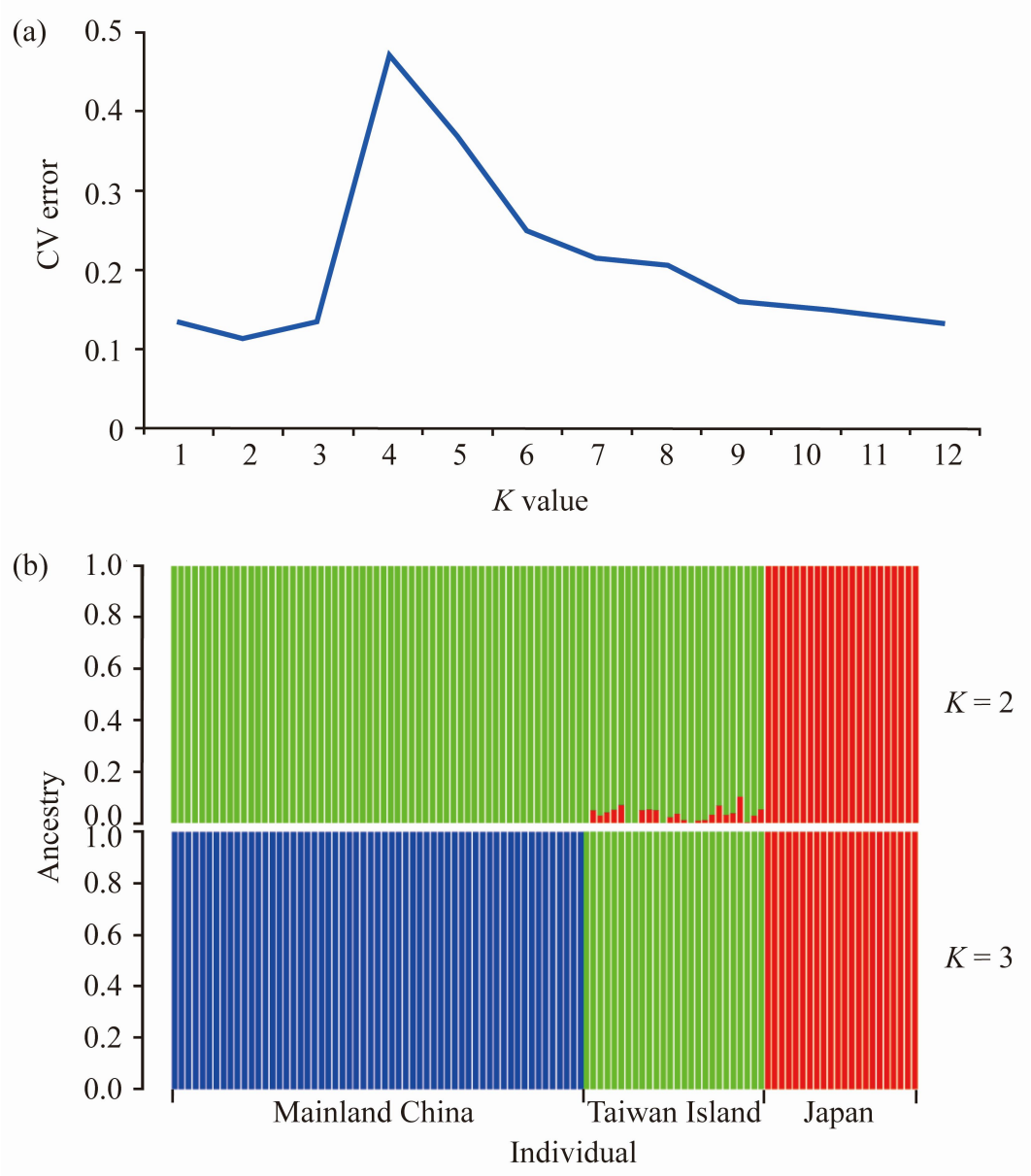


**FIGURE 1** Population genetic structure analysis based on SNP data of *Conandron ramondioides* individuals, as analyzed with ADMIXTURE. (a) Values of CV Error at different *K* values. (b) Clustering situations within all individuals of *C. ramondioides* when $K = 2$ and $K = 3$.

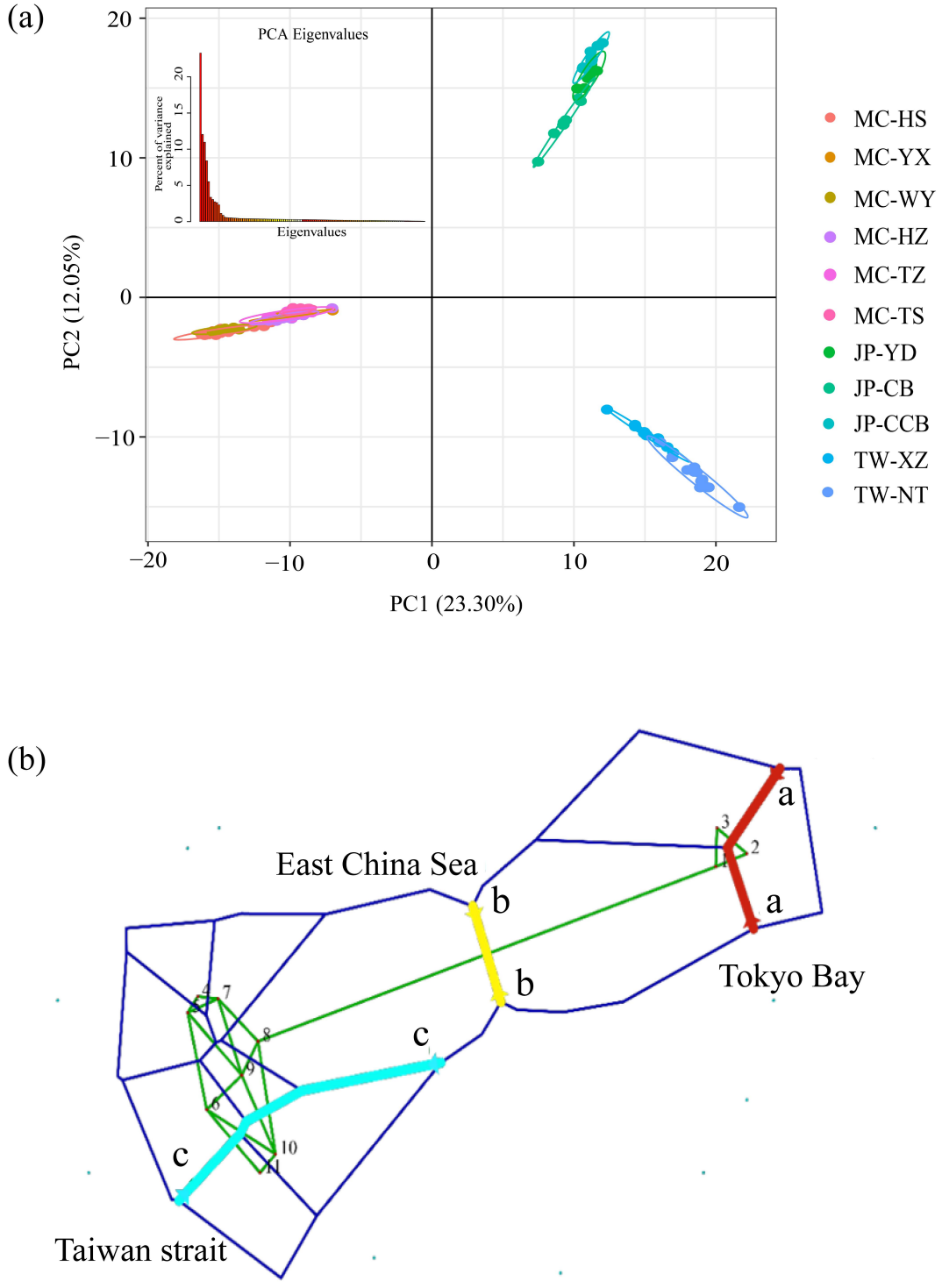


977

978 **FIGURE 2** (a) Principal Component Analysis (PCA) based on SNP data of the 108 studied
979 individuals of *Conandron ramondioides*, with the proportion of the variance explained being
980 23.30% for PC1 and 12.05% for PC2. (b) Major genetic boundaries detected among *C.*
981 *ramondioides* populations using BARRIER v.2.2. The insert figure in A plots the eigenvalues of
982 different principal components.

983

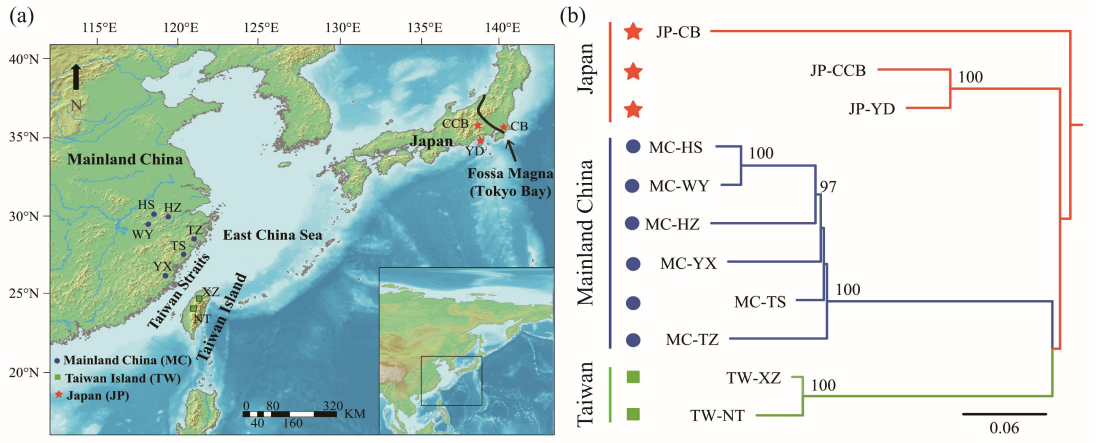


984

985 **FIGURE 3** (a) Map of East Asia showing the studied *Conandron ramondioides* populations with
986 (b) the maximum likelihood phylogenetic tree using the RAD tag SNPs. Node support in the tree
987 is given as the maximum parsimony bootstrap value, bootstrap values below 80% are not
988 indicated. Colored bars and branches identify the three major genetic lineages.

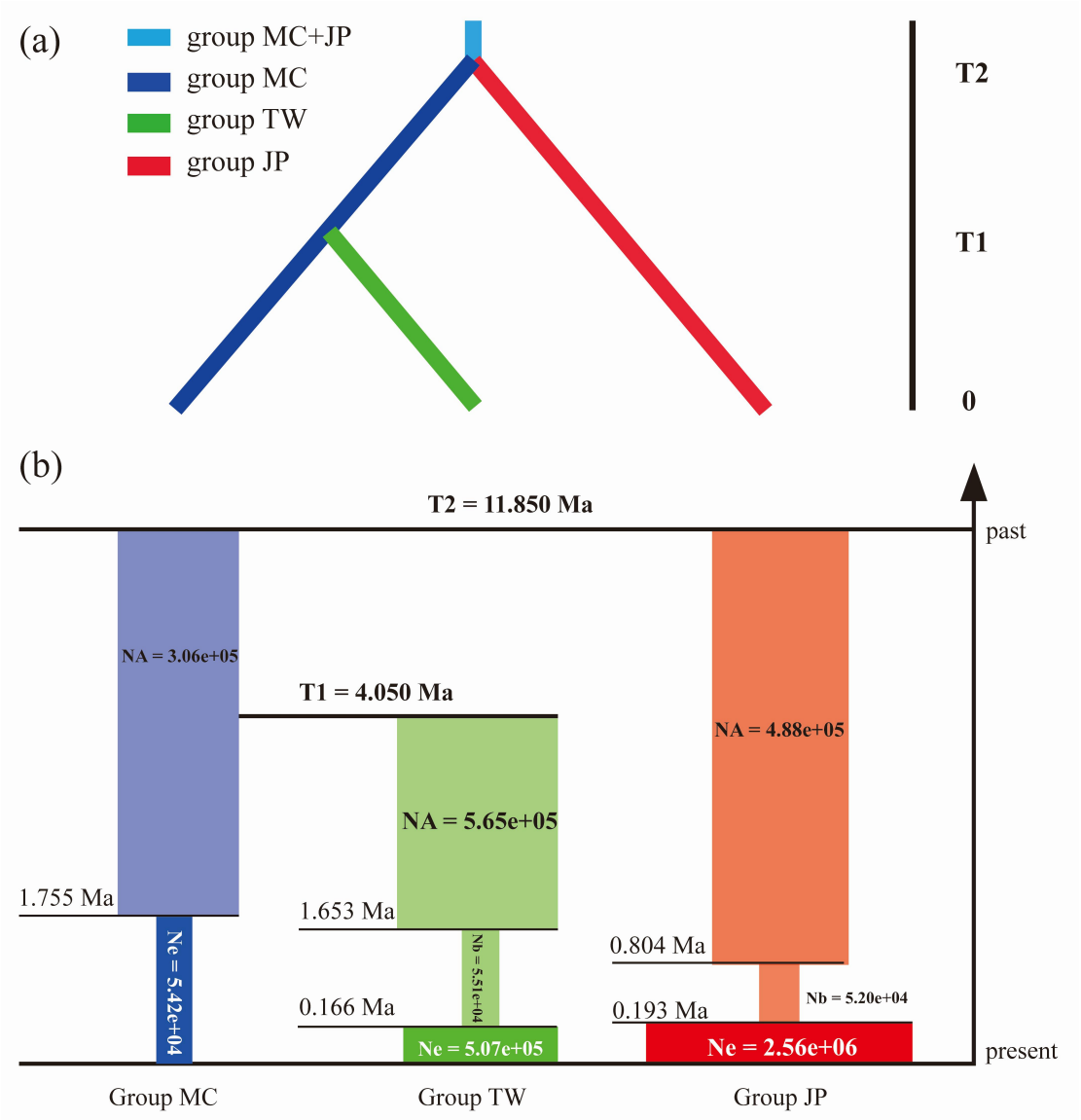


**FIGURE** 4 (a) The best ABC model for *Conandron ramondioides* based on DIYABC analysis; (b) Demographic history of the three groups under the best-fit ABC model. Times of population size changes are indicated by horizontal dashed lines.

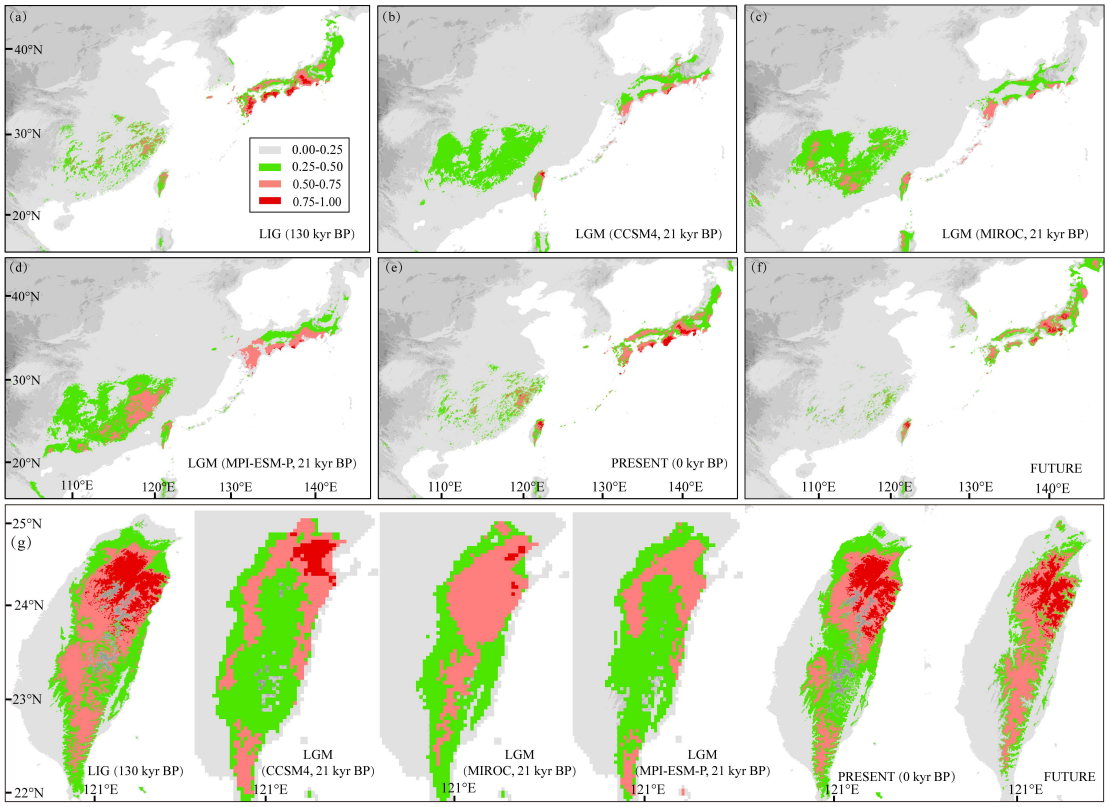


**FIGURE** 5 Results of species distribution modeling (SDM) of *Conandron ramondioides*, represented as predicted distribution probability (as logistic values). (a) Average projection of the model to the Last Interglacial (ca. 120-140 kyr before present (BP)). Average projections of the model to the Last Glacial Maximum (ca. 21 kyr BP) using the (b) CCSM4, (c) MIROC and (d) MPI-ESM-P general circulation model simulations. (e) Predicted distribution for current climatic conditions. (f) Average projections of the model to the future (2070). (g) Zoom of SDMs for Taiwan Island.

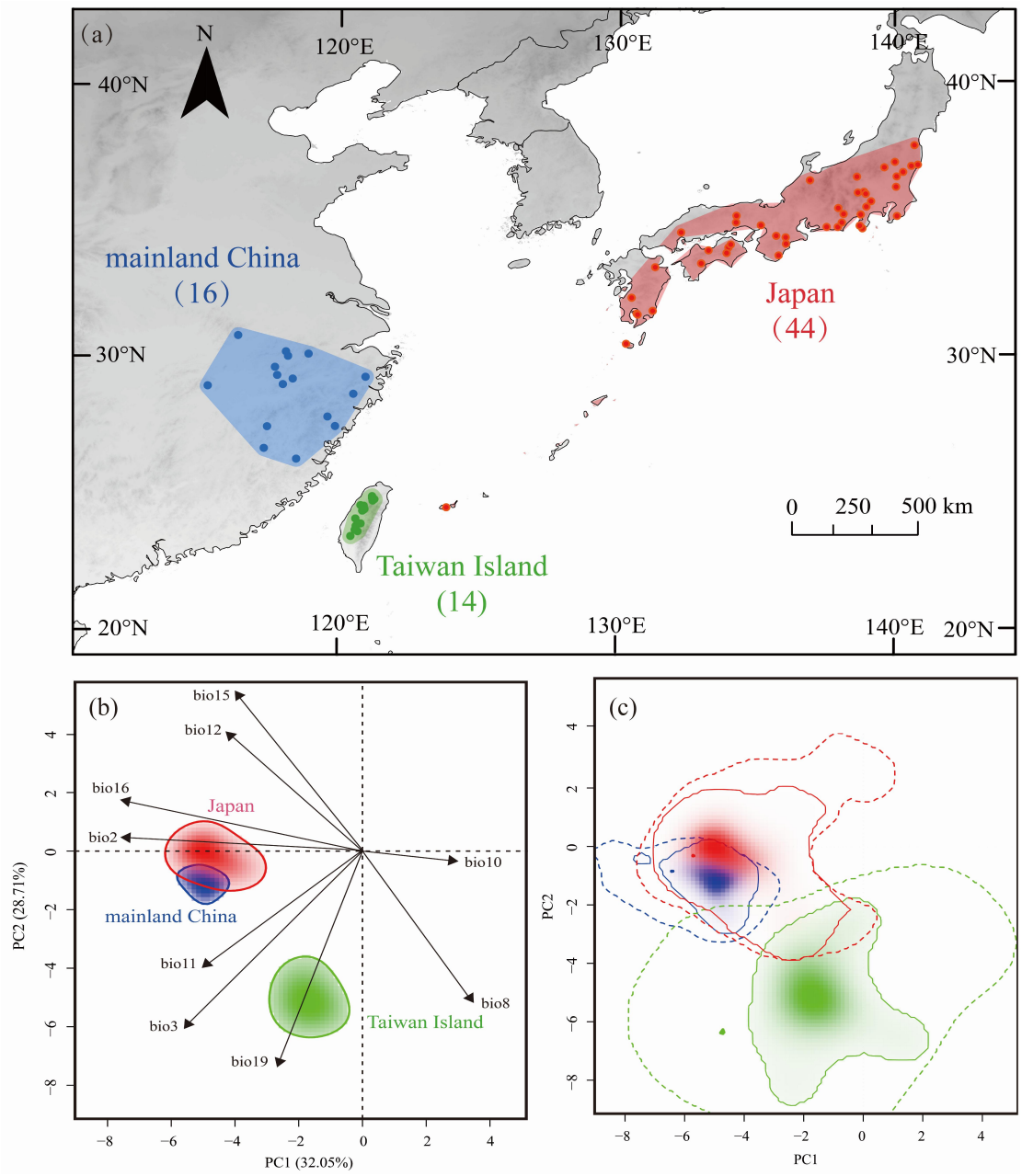


**FIGURE 6** Niche comparisons in environmental space obtained by the environmental niche analysis in RStudio platform. (a) Distributional ranges used for the climatic niche evaluation of *Conandron ramondioides* in mainland China (blue), Taiwan Island (green) and Japan (red). The occurrence records were showed by dots, and colored polygons represented the background areas. The number of occurrences records used for each range were showed below the ranges labels. (b, c) Global climate space, where the three realized niches in a shading gradation scale according to their density of occurrence per cell are projected. (b) The contribution and direction of the nine climatic variables to the first two PCA-env axes are presented, and the solid lines illustrate the 50% of occurrence density. (c) The solid and dashed lines show the 100% occurrences density and the 100% available climatic background, respectively.

1014 **TABLE 1** Collection location, site ID and geographical coordinates of sampled populations of *Conandron ramondioides*. *N*, number of sampled individuals. Prov., province (the first-level administrative division in China); Pref., Prefecture (the first-level administrative division in Japan).

| Code | Location | *N* | Latitude/Longitude | Elevation (m) | Voucher |
|---|---|---|---|---|---|
| JP-YD | Izu Peninsula, Shizuoka Pref., Japan | 7 | N34º41'05"/E138º53'52" | 100 | Ren2018061601 |
| JP-CB | Kiyosumi, Chiba Pref., Japan | 8 | N35º08'37"/E140º08'19" | 90 | Ren2018070201 |
| JP-CCB | Ochigawa, Chichibu, Saitama Pref., Japan | 8 | N36º02'41"/E138º57'13" | 545 | Ren2018072801 |
| MC-HS | Huangshan, Anhui Prov., China | 16 | N30º07'21"/E118º10'31" | 1,158 | - |
| MC-WY | Tuochuan, Wuyuan, Jiangxi Prov., China | 5 | N29º32'47"/E117º46'54" | 821 | Hou2020060301 |
| MC-YX | Youxi, Fujian Prov., China | 7 | N26º08'25"/E118º32'31" | 657 | - |
| MC-HZ | Damingshan, Hangzhou, Zhejiang Prov., China | 13 | N30º02'16"/E118º59'13" | 556 | - |
| MC-TZ | Kuocangshan, Taizhou, Zhejiang Prov., China | 8 | N28º32'40"/E120º35'36" | 710 | Hou2020052501 |
| MC-TS | Wuyanling, Taishun, Zhejiang Prov., China | 10 | N27º21'04"/E119º56'13" | 539 | - |
| TW-XZ | Yuanyang Valley, Xinzhu, Taiwan Prov., China | 11 | N24º34'54"/E121º17'22" | 973 | Ren2019061601 |
| TW-NT | Xitou Nature Park, Nantou, Taiwan Prov., China | 15 | N23º55'11"/E120º40'12" | 1,379 | Ren2019062401 |

**TABLE 2** Genetic diversity statistics within the 11 sampled populations of *Conandron ramondioides*. PA: number of private alleles; %*P* = percent of polymorphic sites,. $H_E$: expected heterozygosity; $H_O$: observed heterozygosity; $\pi$: nucleotide diversity; and $F_{IS:}$ inbreeding coefficient.

| Pop. code | PA | %*P* | $H_E$ | $H_O$ | π | $F_{IS}$ |
|---|---|---|---|---|---|---|
| MC-HS | 279 | 0.976 | 0.042 | 0.029 | 0.030 | -0.021 |
| MC-YX | 497 | 0.973 | 0.045 | 0.033 | 0.036 | -0.016 |
| MC-WY | 286 | 0.973 | 0.049 | 0.031 | 0.036 | -0.024 |
| MC-HZ | 485 | 0.974 | 0.043 | 0.032 | 0.033 | -0.017 |
| MC-TZ | 623 | 0.970 | 0.050 | 0.038 | 0.042 | -0.014 |
| MC-TS | 640 | 0.966 | 0.055 | 0.042 | 0.045 | -0.017 |
| JP-YD | 650 | 0.963 | 0.059 | 0.047 | 0.052 | -0.011 |
| JP-CB | 1302 | 0.966 | 0.054 | 0.043 | 0.047 | -0.011 |
| JP-CCB | 862 | 0.957 | 0.062 | 0.057 | 0.061 | 0.005 |
| TW-XZ | 1080 | 0.965 | 0.051 | 0.048 | 0.051 | 0.005 |
| TW-NT | 882 | 0.969 | 0.046 | 0.040 | 0.042 | -0.001 |
| Average | 688.73 | 0.968 | 0.050 | 0.040 | 0.043 | -0.011 |

1015

**TABLE 3** Analysis of molecular variance (AMOVA) based on SNP data of 108 *Conandron ramondioides* individuals. *df*: degrees of freedom.

| Scale | Source of variation | *df* | Sum of squares | Variance components | Percentage of variation |
|---|---|---|---|---|---|
| Total | Among populations | 10 | 6232.524 | 74.69387 | 83.37 |
| | Within populations | 97 | 1183.551 | 14.89961 | 16.63 |
| | Total | 107 | 7416.075 | 89.59349 | 100.00 |
| Define Groups ($K$ = 2) | Among groups | 1 | 1292.298 | 25.36556 | 24.12 |
| | Among populations within groups | 9 | 4940.226 | 64.89554 | 61.71 |
| | Within populations | 97 | 1183.551 | 14.89961 | 14.17 |
| | Total | 107 | 7416.075 | 105.16071 | 100.00 |
| Define Groups ($K$ = 3) | Among groups | 2 | 3415.62 | 48.70373 | 45.91 |
| | Among populations within groups | 8 | 2816.904 | 42.47085 | 40.04 |
| | Within populations | 97 | 1183.551 | 14.89961 | 14.05 |
| | Total | 107 | 7416.075 | 106.07419 | 100.00 |

1016

**TABLE 4** Selection of major bioclimatic variables used in this study and their contribution rate to the four time periods considered.

| Code | Bioclimatic variable | Contribution rate (%) | | | | | |
|---|---|---|---|---|---|---|---|
| | | LIG | LGM (CCSM4) | LGM (MIROC) | LGM (MPI-ESM-P) | PRESENT | FUTURE |
| Bio 2 | Mean diurnal range (mean of monthly (max temp-min temp)) | 0.2 | 0.8 | 0.4 | 2 | 1.4 | 0.9 |
| Bio 3 | Isothermality | 0.9 | 3.8 | 4.9 | 0.8 | 2 | 2.7 |
| Bio 8 | Mean temperature of wettest quarter | 0.3 | 1 | 0.8 | 0.4 | 0.5 | 0.6 |
| Bio10 | Mean temperature of warmest quarter | 13.6 | 17 | 14.1 | 16.7 | 14.9 | 13.3 |
| Bio11 | Mean temperature of coldest quarter | 0.6 | 0.5 | 0.5 | 0.1 | 0.9 | 0.9 |
| Bio12 | Annual precipitation | 18.2 | 12.2 | 13.8 | 22.9 | 17.3 | 15.8 |
| Bio15 | Precipitation seasonality (coefficient of variation) | 2.8 | 4.3 | 3.2 | 2.5 | 4.5 | 1.9 |
| Bio16 | Precipitation of wettest quarter | 0.1 | 0.4 | 0.2 | 0.2 | 0.1 | 0.1 |
| Bio19 | Precipitation of coldest quarter | 63.2 | 59.9 | 62 | 54.4 | 58.6 | 63.8 |

1017

**TABLE 5** Potential suitable areas of *Conandron ramondioides* in different climate scenarios (× $10^4$ $km^2$).

| Time | Highly suitable area | Moderately suitable area | Lowly suitable area | Total suitable area | Unsuitable area |
|---|---|---|---|---|---|
| LIG | 4.34 | 18.86 | 35.50 | 58.70 | 804.45 |
| LGM (CCSM4) | 0.32 | 5.76 | 68.82 | 74.90 | 790.51 |
| LGM (MIROC) | 0.09 | 13.27 | 68.52 | 81.88 | 783.54 |
| LGM (MPI-ESM-P) | 0.36 | 26.48 | 71.30 | 98.14 | 767.27 |
| PRESENT | 2.60 | 14.76 | 27.84 | 45.20 | 817.94 |
| FUTURE | 1.41 | 11.07 | 23.41 | 35.89 | 827.25 |

1018

**TABLE 6** Area changes in suitable habitat area for *Conandron ramondioides* in different climate scenarios (× $10^4$ $km^2$).

| Climate scenario | range expansion | no occupancy (absence in both) | no change (presence in both) | range contraction |
|---|---|---|---|---|
| LGM (CCSM4)–LIG | 1.35 | 701.53 | 3.71 | 17.13 |
| LGM (MIROC)–LIG | 6.14 | 696.74 | 6.17 | 14.66 |
| LGM (MPI)–LIG | 12.04 | 690.84 | 12.47 | 8.36 |
| PRESENT–LIG | 0.41 | 706.20 | 15.41 | 5.83 |
| PRESENT–LGM (CCSM4) | 12.06 | 706.60 | 3.41 | 1.65 |
| PRESENT–LGM (MIROC) | 10.55 | 700.84 | 4.92 | 7.39 |
| PRESENT–LGM (MPI) | 5.57 | 693.63 | 9.90 | 14.61 |
| FUTURE–PRESENT | 3.41 | 708.61 | 7.68 | 8.15 |

1019

**Table 7** Paired niche comparisons between the three distribution ranges examined: *Conandron ramondioides* from mainland China, Taiwan Island and Japan. Schoener's *Ds* indicates the niche overlap level between realized climatic niches, 0 = no overlap, 1 = complete overlap. The niche equivalency (eq) and niche similarity (sim) tests are significant ($P < 0.05$) when niche overlap is smaller than randomly expected (niche divergence; D), or larger than randomly expected (niche conservation; C). The three niche dynamic parameters (unfilling, stability, expansion) are also shown.

| Distribution ranges (comparisons *1* → *2*) | | Niche Overlap (*Ds*) | Equivalency test (*P*-value) | | Similarity test (*P*-value) | | Niche unfilling | Niche stability | Niche expansion |
|---|---|---|---|---|---|---|---|---|---|
| *1* | *2* | | less eq | more eq | less sim | more sim | | | |
| mainland China | Japan | 0.201 | 0.158 | 0.762 | 0.871 | 0.198 | 0.048 | 0.371 | 0.629 |
| | Taiwan Island | 0 | **0.01D** | 1 | 0.713 | 1 | 1 | 0 | 1 |
| Japan | mainland China | 0.201 | 0.277 | 0.743 | 0.861 | 0.149 | 0.629 | 0.952 | 0.048 |
| | Taiwan Island | 0.128 | **0.03D** | 0.99 | 0.881 | 0.168 | 0.931 | 0.119 | 0.881 |
| Taiwan Island | mainland China | 0 | **0.01D** | 1 | 0.713 | 1 | 1 | 0 | 1 |
| | Japan | 0.128 | **0.03D** | 1 | 0.891 | 0.119 | 0.881 | 0.069 | 0.931 |

## Supplementary figures

FIGURE S1: ML phylogenetic tree obtained with by RAxML (Stamatakis et al., 2006), based on SNP data of *Conandron ramondioides* individuals, with three outgroups of *Ridleyandra* sp.. Numeric values indicate branch bootstrap support.

FIGURE S2: Relationship between genetic and geographic distance for *Conandron ramondioides* based on SNP data from 11 populations.

FIGURE S3: (A) Divergence scenarios and corresponding posterior probabilities of *Conandron ramondioides* from DIYABC. In scenario 1, group TW was originated from group MC and diverged at T1, group MC was originated from group JP (ancestral population) and diverged at T2; In scenario 2, group TW was originated from group MC and diverged at T1, group JP was originated from group MC (ancestral population) and diverged at T2; In scenario 3, group MC was originated from group TW and diverged at T1, group JP was originated from group TW (ancestral population) and diverged at T2; In scenario 4, group TW was originated from group MC and diverged at T1, group MC and group JP were originated from group MC+JP (ancestral population) and diverged at T2; In scenario 5, group MC was originated from group TW and diverged at T1, and group TW and group JP were originated from group TW + JP (ancestral population) and diverged at T2; In scenario 6, group MC and group TW were originated from group MC + TW (ancestral

population) and diverged at T1, group MC + TW and group JP were originated from group MC + TW +JP (ancestral population)

and diverged at T2. (B) Four demographic scenarios of changes in population size of Conandron ramondioides. NA and Na, ancestral population size; Ne, current population size; NB and Nb, population sizes between NA and Ne with NA<NB, NA>Ne, Nb<Ne, Na<Ne, t2>t1. (C) Prior and posterior distribution of parameters of best-fit scenarios for demographic history of (a) group MC, (b) group TW and (c) group JP. (D) Plots for fitness of competing and modeling checking for (a) group MC, (b) group TW and (c) group JP based on direct logistic regression, simulated in DIYABC.

FIGURE S4: Receiver operator characteristic curve tests the accuracy of Maxent model in (a) LIG, (b) LGM (CCSM4), (c) LGM (MIROC), (d) LGM (MPI-ESM-P), (e) PRESENT and (f) FUTURE (2070).

FIGURE S5: Jackknife test for the significance of bioclimatic variables performed by MaxEnt model in (a) LIG, (b) LGM (CCSM4), (c) LGM (MIROC), (d) LGM (MPI-ESM-P), (e) PRESENT and (f) FUTURE (2070).